Diffraction, ultra-peripheral collisions, low x physics at the LHC and connection to EIC

- intro
- gluons, low x phenomena, and saturation
- diffraction and deep inelastic scattering at HERA
- diffraction at the LHC
- UPC and low x physics
- forward charm and low x gluons
- connection to EIC physics

EMMI seminar, GSI
Wed., Oct. 25, 2017

UNIVERSITÄT
HEIDELBERG
ZUKUNFT
SEIT 1386

recent reference on the physics of saturation:

IOP Publishing

Reports on Progress in Physics

Rep. Prog. Phys. **80** (2017) 032301 (33pp)

doi:10.1088/1361-6633/aa5435

Key Issues Review

High gluon densities in heavy ion collisions

Jean-Paul Blaizot

Institut de Physique Théorique, CNRS/UMR 3681, CEA Saclay, F-91191 Gif-sur-Yvette, France

parton distribution functions as a function of the momentum fraction x of the nucleon

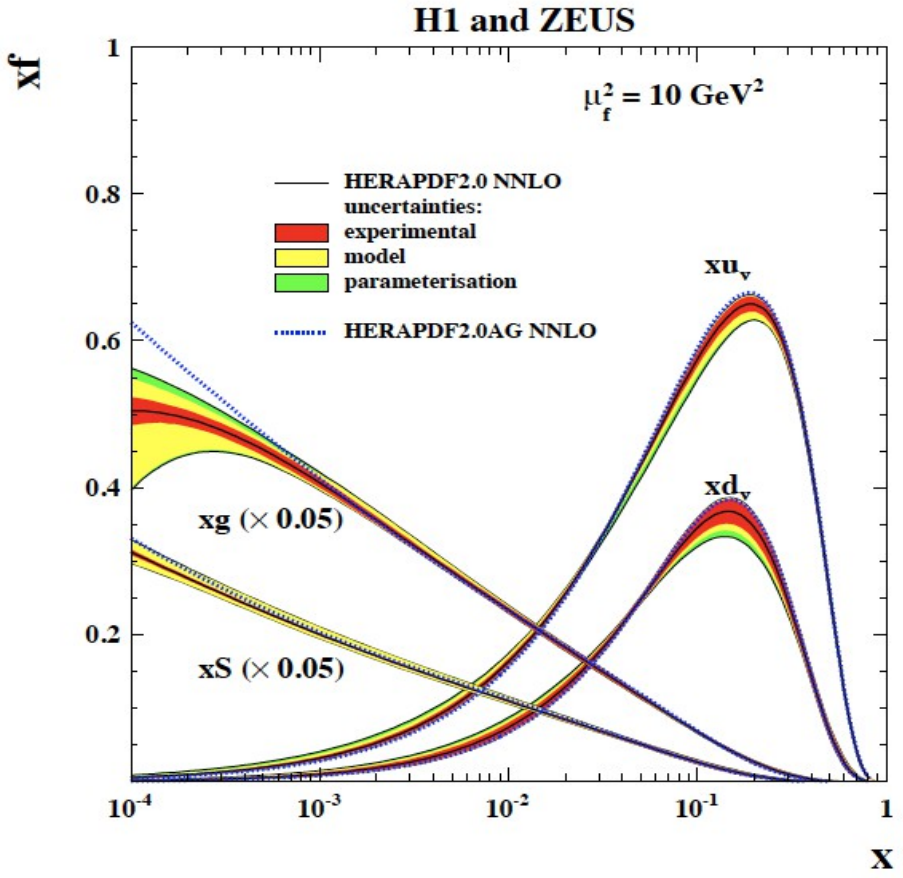

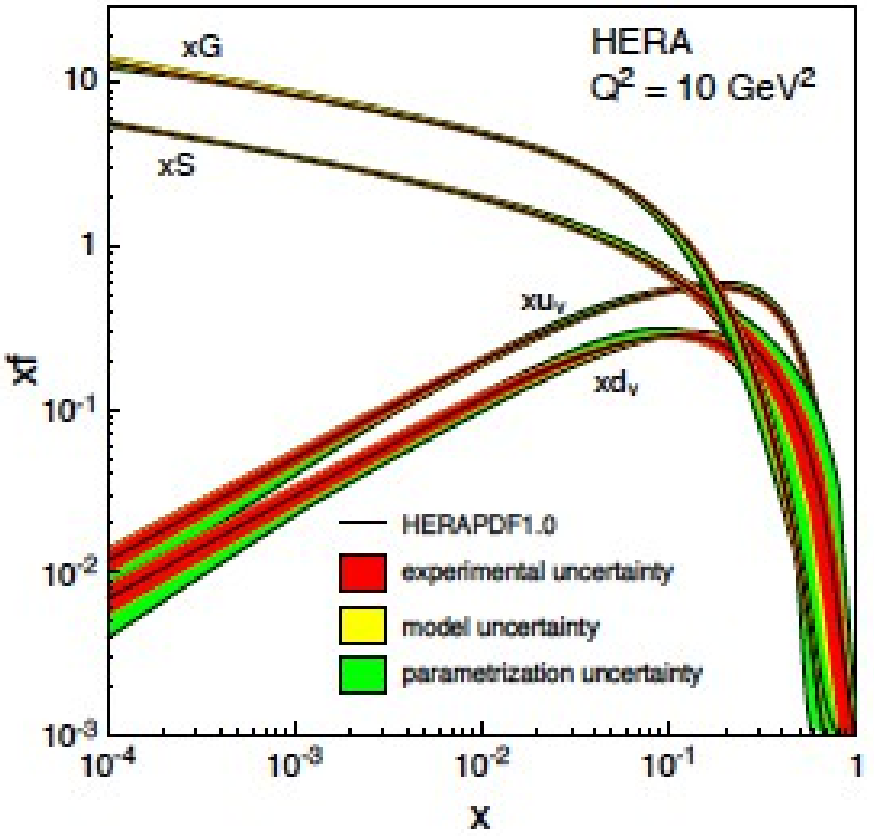

for $x < 10^{-2}$, gluons completely dominate
the wave function of hadrons

variables in deep inelastic scattering

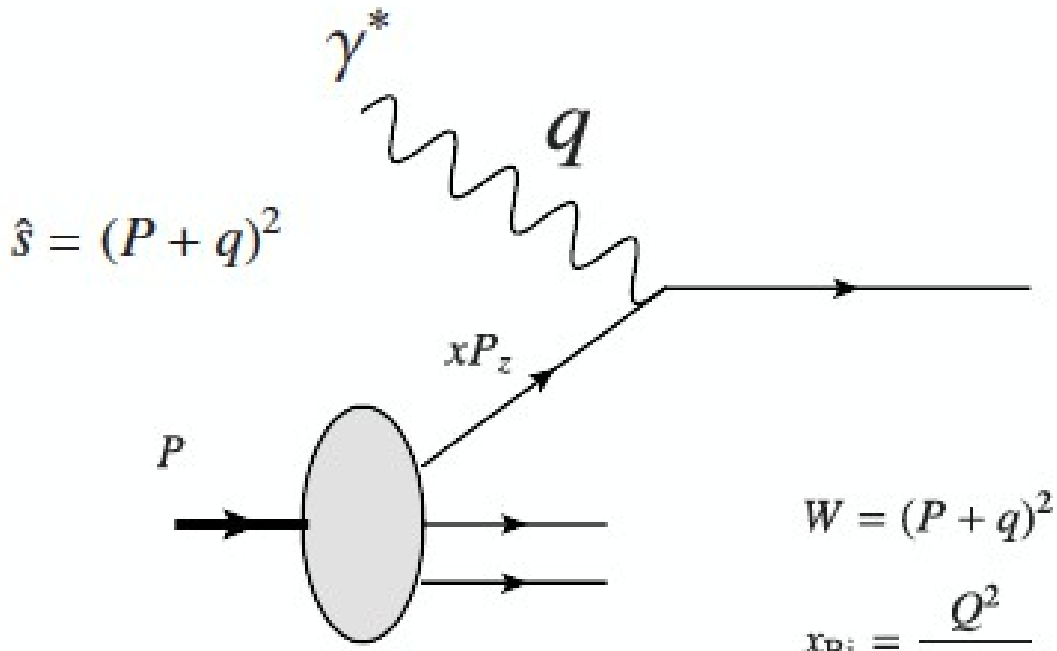

$$W = (P+q)^2$$

$$x_{\mathrm{Bj}} = \frac{Q^2}{2P \cdot q}$$

$$Q^2 = -q^2$$

$Q^2 \gg \Lambda^2_{QCD}$ perturbative

$x \approx \frac{Q^2}{\hat{s}} \ll 1$ 'low x region'

June 23, 2014

Saturation scale

$x \cdot G(x, Q^2) = \alpha_s \frac{C_F}{\pi} \ln\left(\frac{Q^2}{\Lambda_{QCD}^2}\right)$

gluon dist.

$= \int_{\Lambda^2_{QCD}}^{Q^2} dk_\perp^2 \frac{1}{k_\perp^2} \cdot \varphi(x, k_\perp)$

Unintegrated gluon distribution

Saturation momentum

$Q_s^2 = \alpha_s(Q_s^2) \times G(x, Q_s^2) \cdot \frac{1}{\pi R^2}$

Nuclei in purely geometric

If $x \cdot G(x, Q_s^2) \sim A$ then

$Q_s^2 \sim A^{1/3}$ bit

(a) what is the role of 'shadowing' in this?

(b) why is radius of nucleus there, why not transverse expansion of area?

alternatively: $\frac{\pi}{Q_s^2} \cdot x G(x, Q_s^2) \cdot \frac{N_s}{\pi} = \pi R^2$

transverse size of gluon

number of gluons

encourage

the saturation momentum Q_s separates the low gluon density region from the high gluon density region

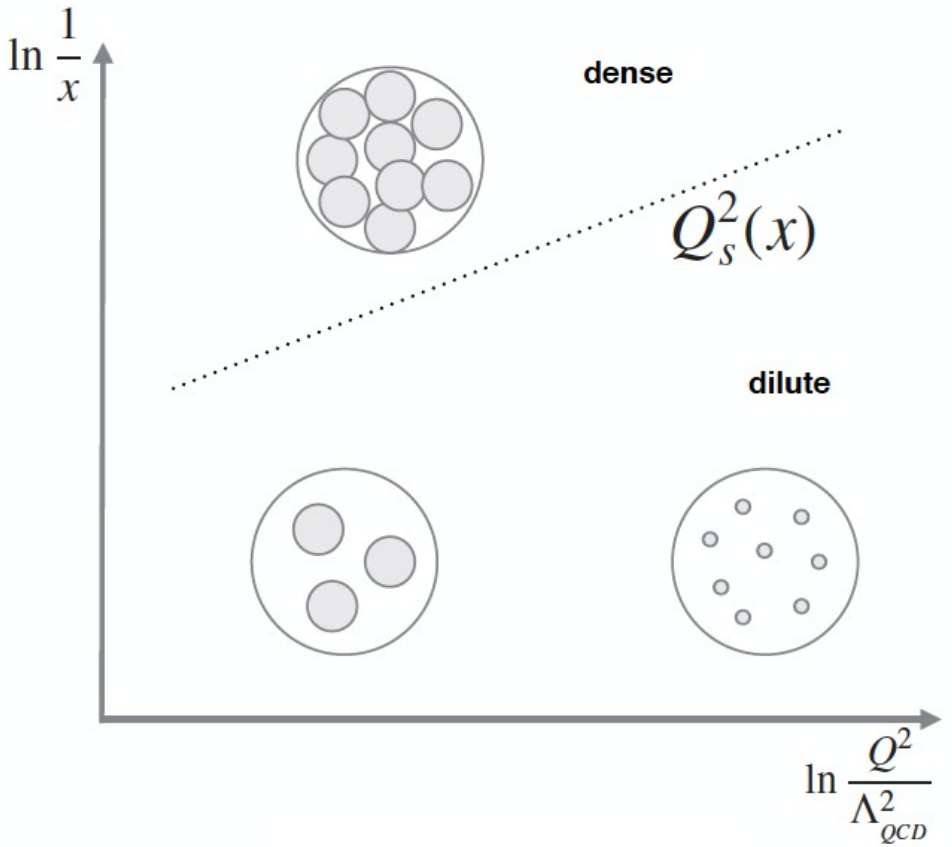

$$Q_s^2 \sim \alpha_s(Q_s^2)\frac{xG(x,Q_s^2)}{\pi R^2}$$

$$Q_s^2(x) \sim A^{1/3}\left(\frac{1}{x}\right)^{\lambda} \qquad \lambda = 0.2 - 0.3$$

$$Q_s^2(x) \sim \left(\frac{A}{x}\right)^{1/3}$$

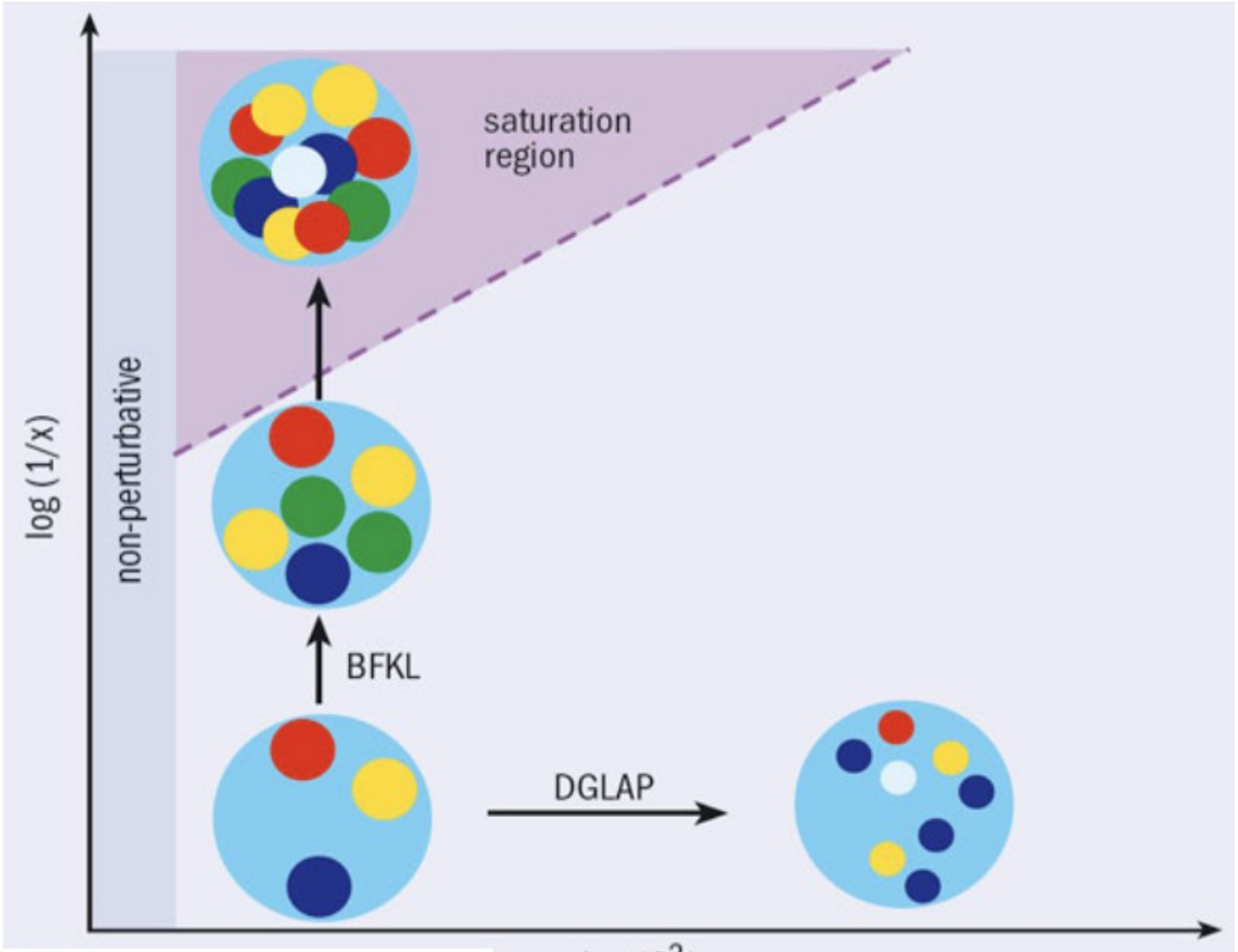

Diagram from CERN Courier

saturation momentum for a
Au nucleus (A = 197)
at a given x is as large as that for a proton at
an x scale reduced by a factor 197

can one see saturation effects in particle production experiments?

energy dependence of hadron production in central Pb-Pb (Au-Au) collisions

total number of hadrons produced

2.76 TeV
N_had = 25800

5.02 TeV
N_had = 32300

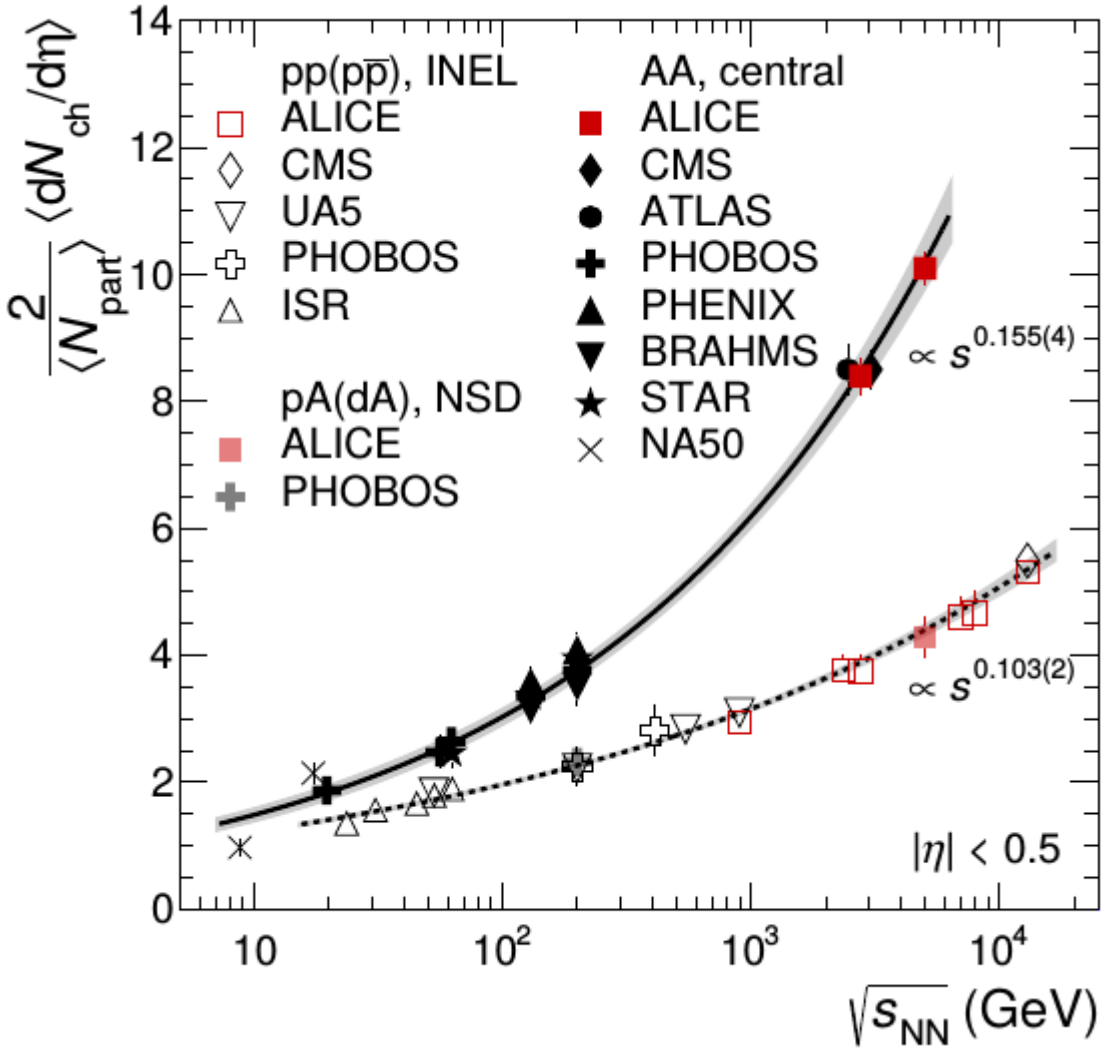

data from LHC run1 and run2

ALICE coll., Phys.Rev.Lett. 116 (2016) no.22, 222302

note: exponent in energy dependence is different for pp and PbPb; not anticipated but now explained in saturation models

energy dependence of particle production in Pb-Pb collisions at LHC

QCD saturation at the LHC: comparisons of models to p+p and A+A data and predictions for p+Pb collisions

Prithwish Tribedy[1] and Raju Venugopalan[2]

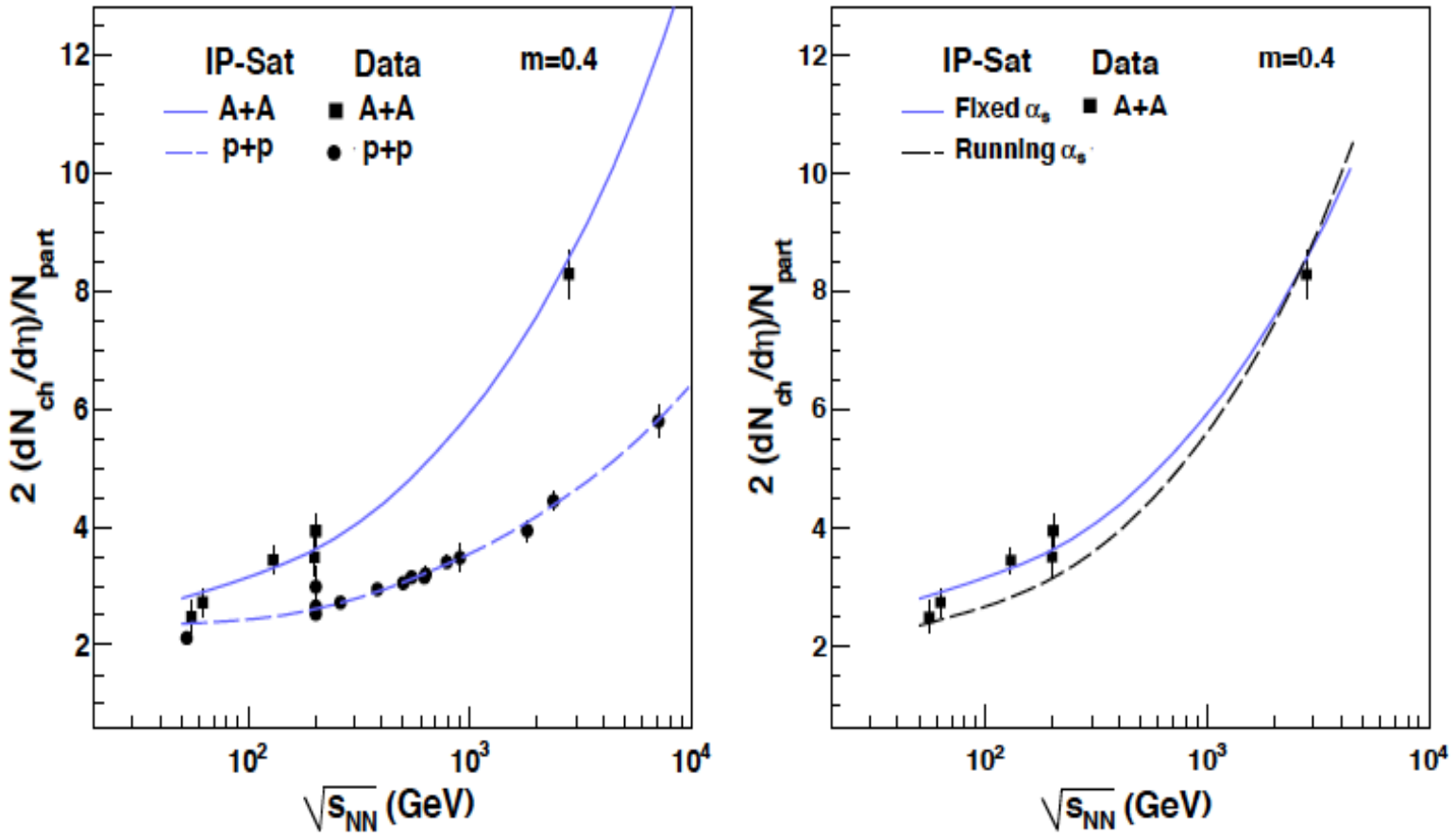

The difference between pp and Pb-Pb is explained as due to the larger scaling violations in a large nucleus compared to the pp case, arXiv:1112.2445

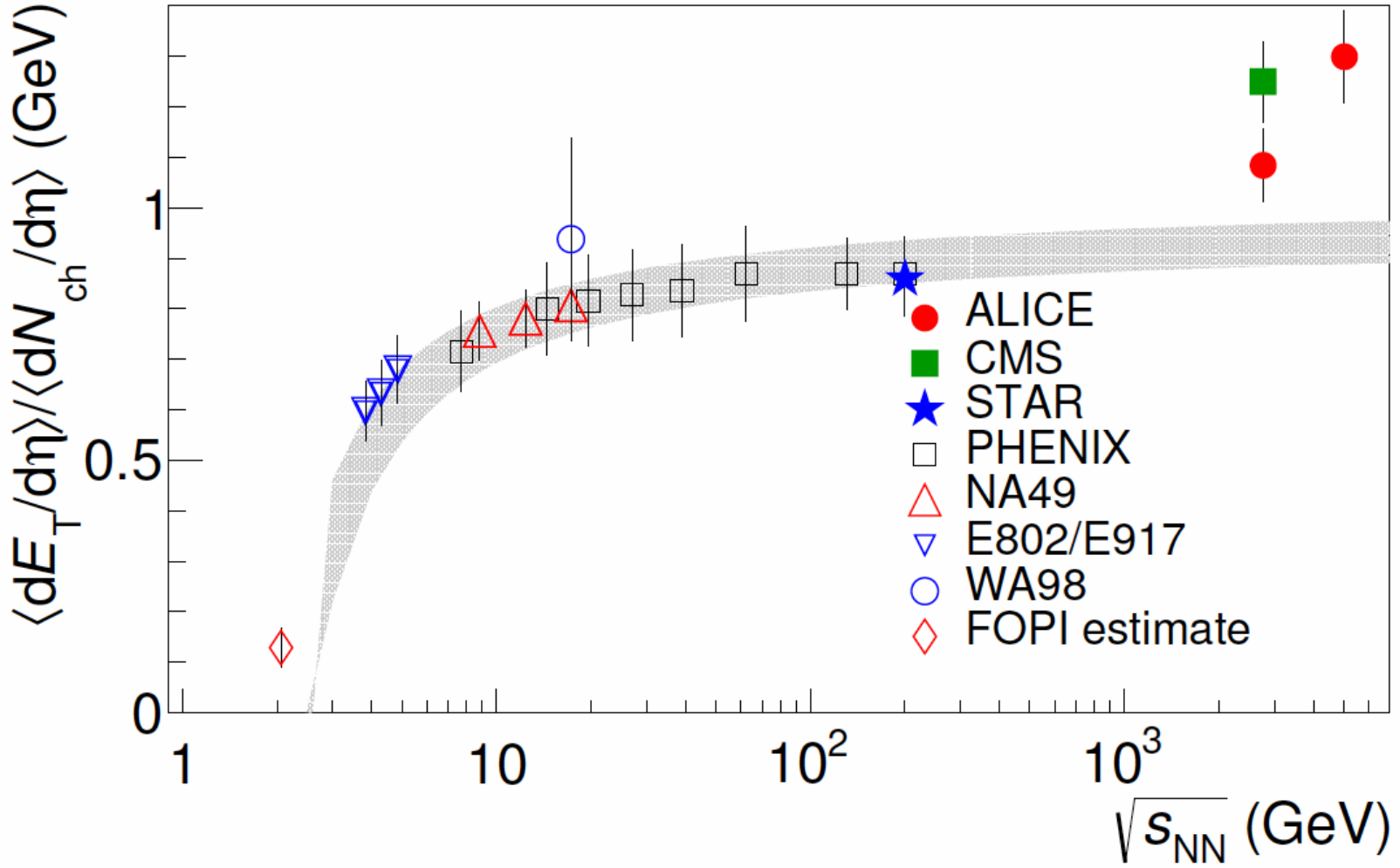

indication of anomalous energy dependence?

energy dependence of transverse energy distribution

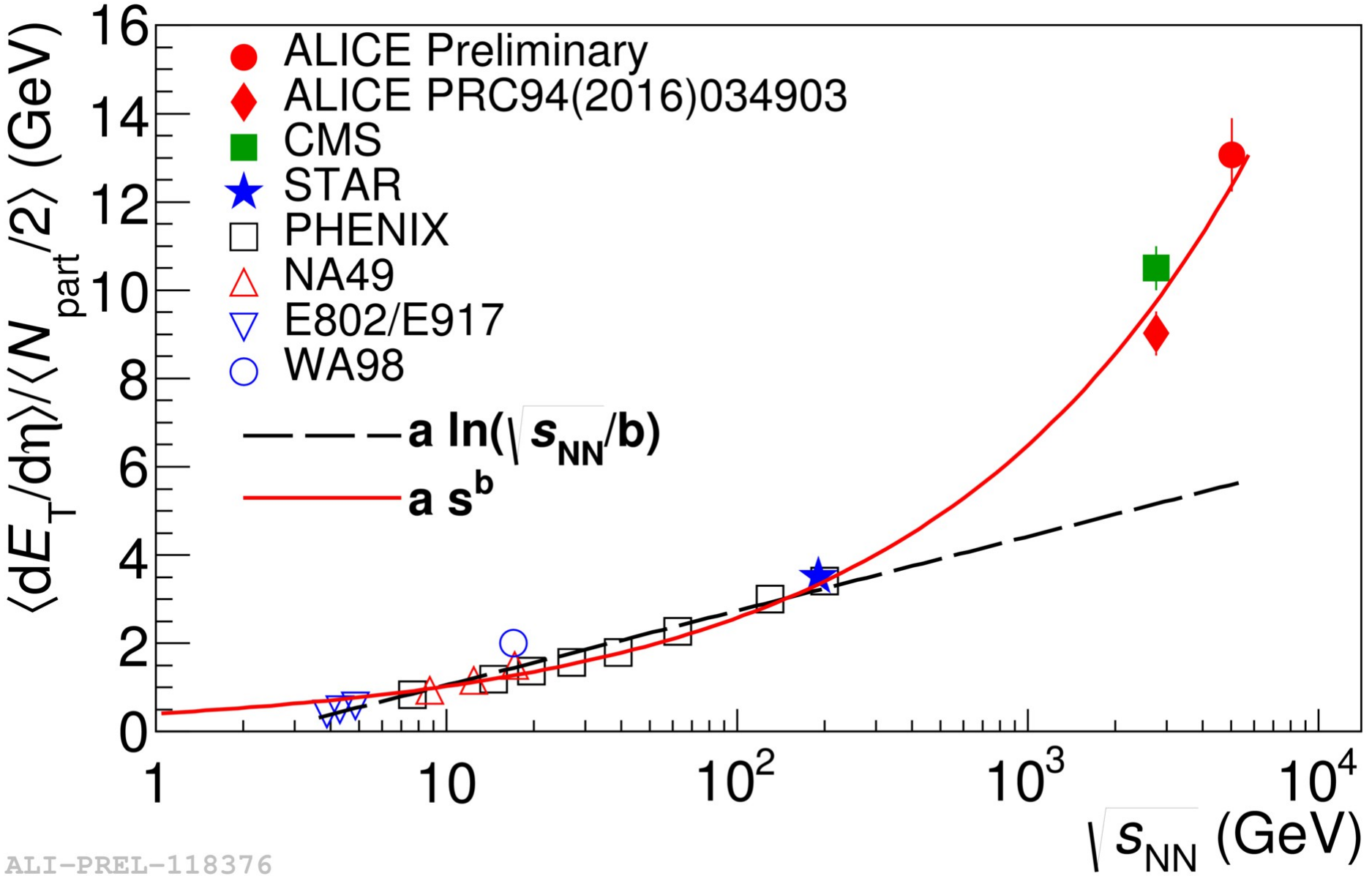

ALI-PREL-118376

note: a s^b = 0.4 s^0.2

N_{ch} and E_T cannot directly be obtained in a perturbative approach

look for other observables:
charmonium production in diffractive and ultra-peripheral collisions

charmonium production in diffractive events at HERA

1st order perturbation theory,
Jones, Martin, Ryskin, Teubner, JHEP 1311 (2013) 085,

including higher orders,
J.Phys. G43 (2016) no.3, 035002, Eur.Phys.J. C76 (2016) no.11, 633

$$\frac{\mathrm{d}\sigma}{\mathrm{d}t}\left(\gamma^* p \to J/\psi\, p\right)\Big|_{t=0} = \frac{\Gamma_{ee} M_{J/\psi}^3 \pi^3}{48\alpha}\left[\frac{\alpha_s(\bar{Q}^2)}{\bar{Q}^4} x g(x,\bar{Q}^2)\right]^2 \left(1+\frac{Q^2}{M_{J/\psi}^2}\right).$$

Here Γ_{ee} is the electronic width of the J/ψ, and

$$\bar{Q}^2 = (Q^2 + M_{J/\psi}^2)/4, \qquad x = (Q^2 + M_{J/\psi}^2)/(W^2 + Q^2).$$

because of the large mass of the J/psi, the scale Q_bar is large → perturbative approach

2 options, option a not consistent with measured energy dependence

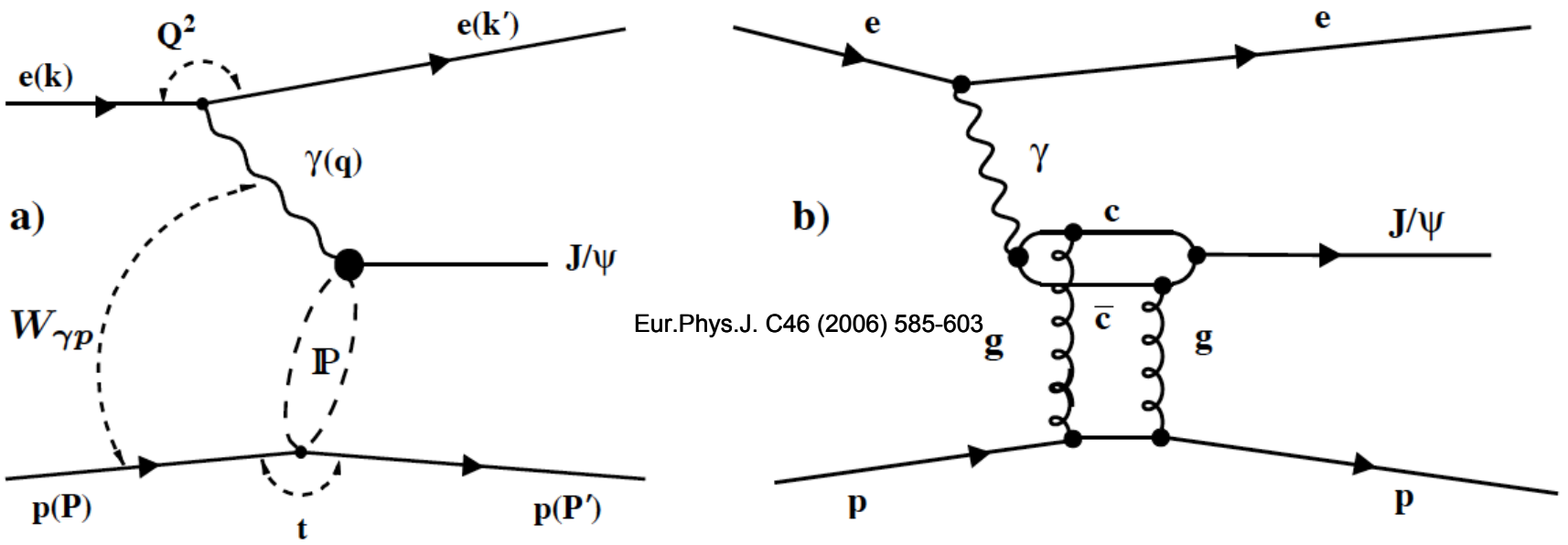

Eur.Phys.J. C46 (2006) 585-603

Figure 1: Elastic J/ψ production, a) in an approach based on Pomeron (IP) exchange and b) in a pQCD approach via two gluon exchange. The kinematic variables are indicated in a).

Hera H1 publication, hep-ex/0510016, Eur.Phys.J. C46 (2006) 585-603

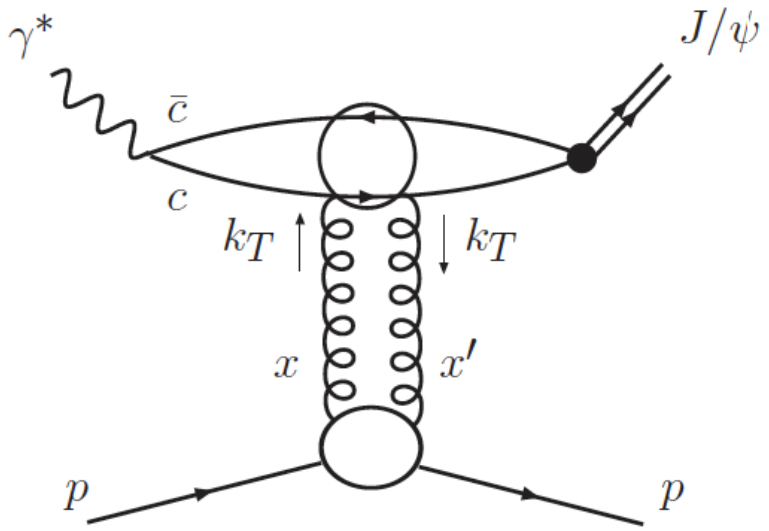

Figure 1: Schematic picture of high energy exclusive J/ψ production, $\gamma^* p \to J/\psi\, p$. The factorised form follows since, in the proton rest frame, the formation time $\tau_f \simeq 2E_\gamma/(Q^2+M^2_{J/\psi})$ is much greater than the $c\bar{c}$-proton interaction time $\tau_{\rm int}$. In the case of the simple two-gluon exchange shown here, $\tau_{\rm int} \simeq R_p$, where R_p is the radius of the proton.

correction for higher orders, see Jones et al.

$$\left[\frac{\alpha_s(\bar{Q}^2)}{\bar{Q}^4} xg(x,\bar{Q}^2)\right] \longrightarrow \int_{Q_0^2}^{(W^2-M_{J/\psi}^2)/4} \frac{\mathrm{d}k_T^2\,\alpha_s(\mu^2)}{\bar{Q}^2(\bar{Q}^2+k_T^2)} \frac{\partial\left[xg(x,k_T^2)\sqrt{T(k_T^2,\mu^2)}\right]}{\partial k_T^2} + \ln\left(\frac{\bar{Q}^2+Q_0^2}{\bar{Q}^2}\right)\frac{\alpha_s(\mu_{\mathrm{IR}}^2)}{\bar{Q}^2 Q_0^2} xg(x,Q_0^2)\sqrt{T(Q_0^2,\mu_{IR}^2)}\,.$$

Hera results from H1 and Zeus

here, $Q^2 = p_t^2$

data parametrized as $\sigma \propto W_{\gamma p}^{\delta}$
W is photon proton cm energy

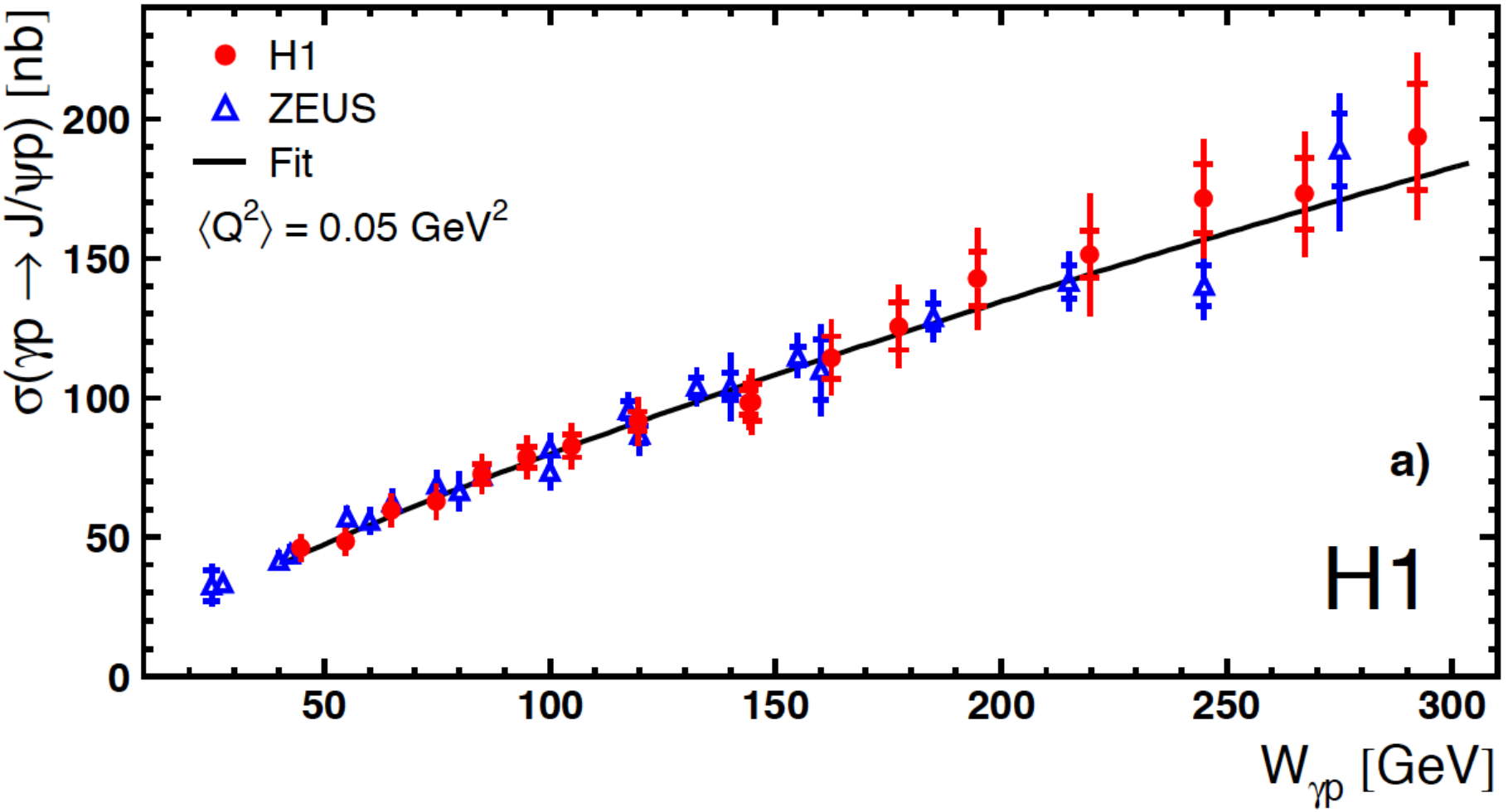

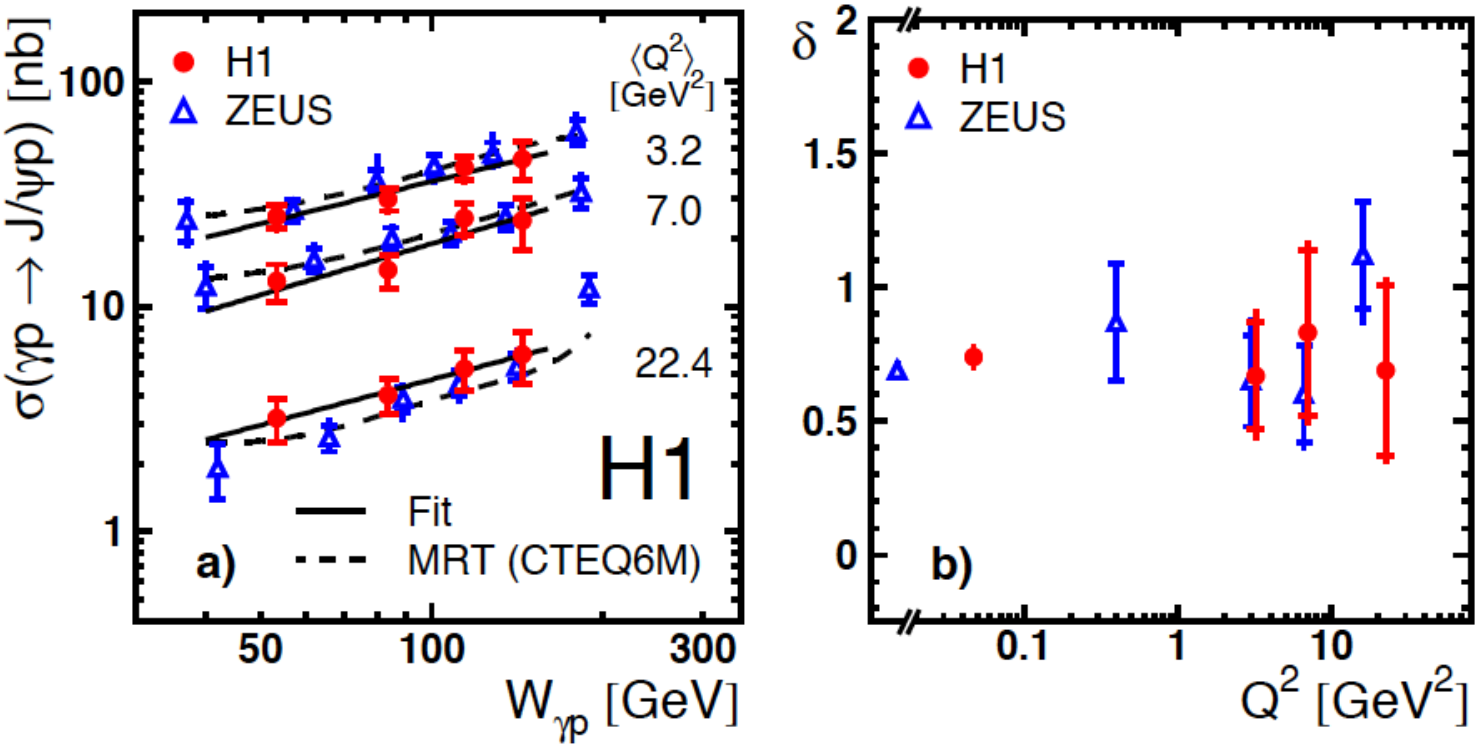

Figure 6: a) Total cross sections for elastic J/ψ production as a function of $W_{\gamma p}$ in the range $|t| < 1.2\,\mathrm{GeV}^2$ in electroproduction in three bins of Q^2. $\langle Q^2 \rangle$ indicates the bin centre value in the Q^2 range considered. The solid lines show fits to the H1 data of the form $\sigma \propto W_{\gamma p}^{\delta}$. The dashed curves show the MRT QCD prediction based on the gluon distribution CTEQ6M [48] with the normalisation factors from the fit to the Q^2 distribution. Results from the ZEUS experiment [16] in a similar kinematic range are also shown. They have been scaled to the given $\langle Q^2 \rangle$ values using the Q^2 dependence measured by ZEUS. b) The fit parameter δ as a function of Q^2. The inner error bars show the statistical error, while the outer error bars show the statistical and systematic uncertainties added in quadrature.

data well described by 'conventional' pQCD calculations

the legacy of HERA deep inelastic scattering data

Does Nature Know about Pertubation Theory?
A Study of HERA Deep Inelastic Scattering Data at Low Q^2

I. Abt[a], A.M. Cooper-Sarkar[b], B. Foster[b,c,d], V. Myronenko[d],
K. Wichmann[d], M. Wing[e]

arXiv:1704.03187

HERA ep deep inelastic scattering data exhibit no unambiguous signs of saturation

1704.03187

A phenomenological study of the final combined HERA data on inclusive deep inelastic scattering (DIS) has been performed. The data are presented and investigated for a kinematic range extending from values of the four-momentum transfer, Q^2, above $10^4\,\mathrm{GeV}^2$ down to the lowest values observable at HERA of $Q^2 = 0.045\,\mathrm{GeV}^2$ and Bjorken x, $x_{\mathrm{Bj}} = 6 \cdot 10^{-7}$. The data are well described by fits based on perturbative quantum chromodynamics (QCD) using collinear factorisation and evolution of the parton densities encompassed in the DGLAP formalism from the highest Q^2 down to Q^2 of a few GeV^2. The Regge formalism can describe the data up to $Q^2 \approx 0.65\,\mathrm{GeV}^2$. The complete data set can be described by a new fit using the ALLM parameterisation. The region between the Regge and the perturbative QCD regimes is of particular interest.

The investigations presented in this paper focus on the e^+p NC data, taken at centre-of-mass energies, $\sqrt{s}$, of 318 GeV and 300 GeV. Their kinematic range spans six orders of magnitude in x_{Bj} and Q^2, on a grid with $6.21 \cdot 10^{-7} \leq x_{\mathrm{Bj}} \leq 0.65$ and $0.045 \leq Q^2 \leq 30000\,\mathrm{GeV}^2$. The corresponding range of the energy available at the photon–proton vertex, $W^2 = Q^2(1/x_{\mathrm{Bj}} - 1) + m_p^2$, where m_p is the mass of the proton, is $10.7 \leq W \leq 301.2\,\mathrm{GeV}$.

While the regime that can be treated by pQCD is clearly limited by theoretical considerations, the data themselves show no abrupt change in behaviour in this regime. Scaling violations are well established and well described by pQCD. The slope, $d\sigma_{r,\mathrm{NC}}/dQ^2$, changes from negative to positive as x_{Bj} decreases. Of particular interest are x_{Bj} values with entries above and below $Q^2 = 1\,\mathrm{GeV}^2$, such as $x_{\mathrm{Bj}} = 0.0008$ and $x_{\mathrm{Bj}} = 0.0032$. The Q^2 dependence does not change in any abrupt way around $Q^2 = 1\,\mathrm{GeV}^2$. It seems that nature does not know about perturbation theory.

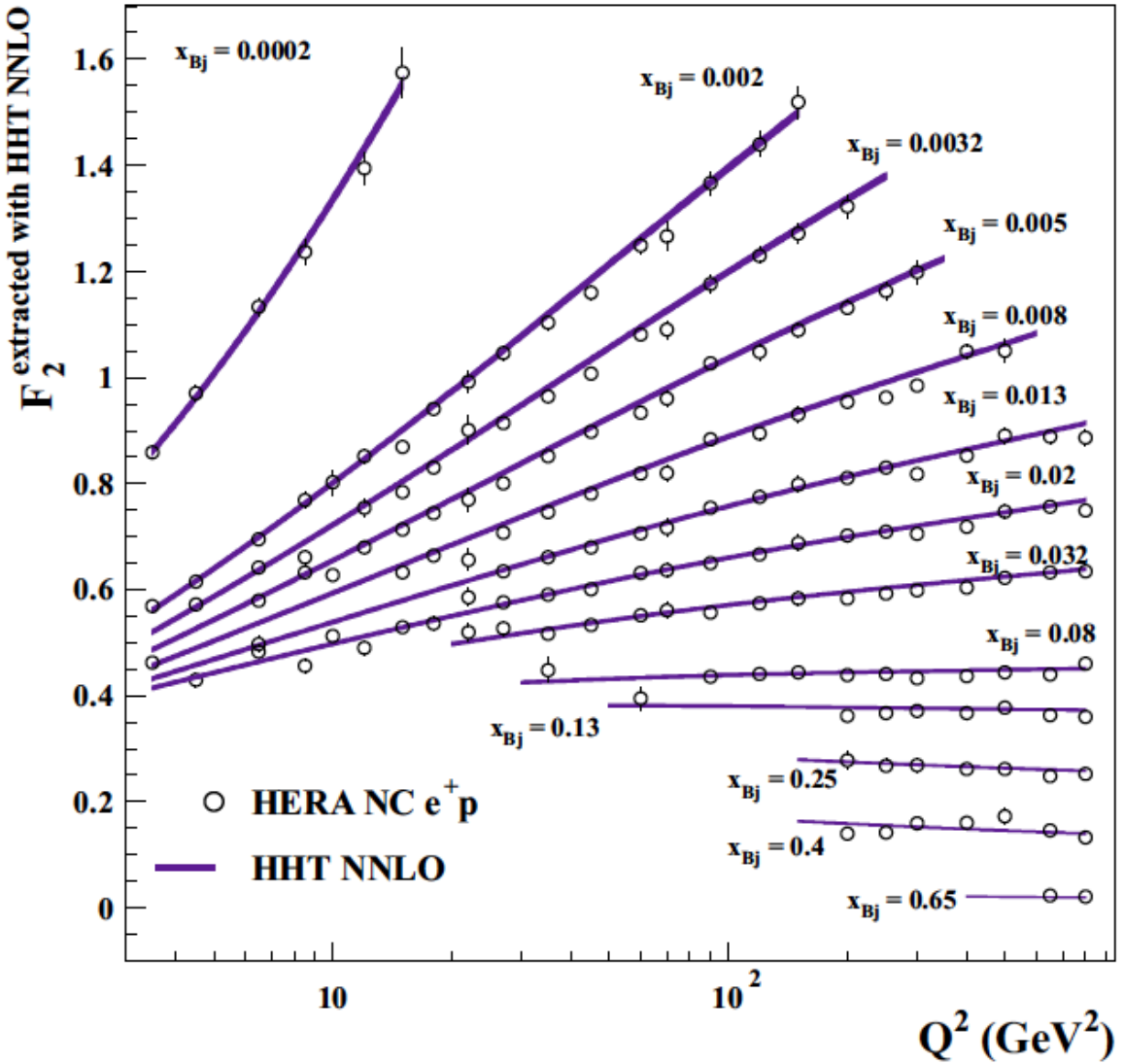

Figure 11: The structure-function $F_2(Q^2)$ for selected values of x_{Bj} in the Q^2-range where F_2 can be extracted within the framework of pQCD using the HHT NNLO analysis. Also shown are the predictions from HHT NNLO. The width of the bands represents the uncertainty on the predictions.

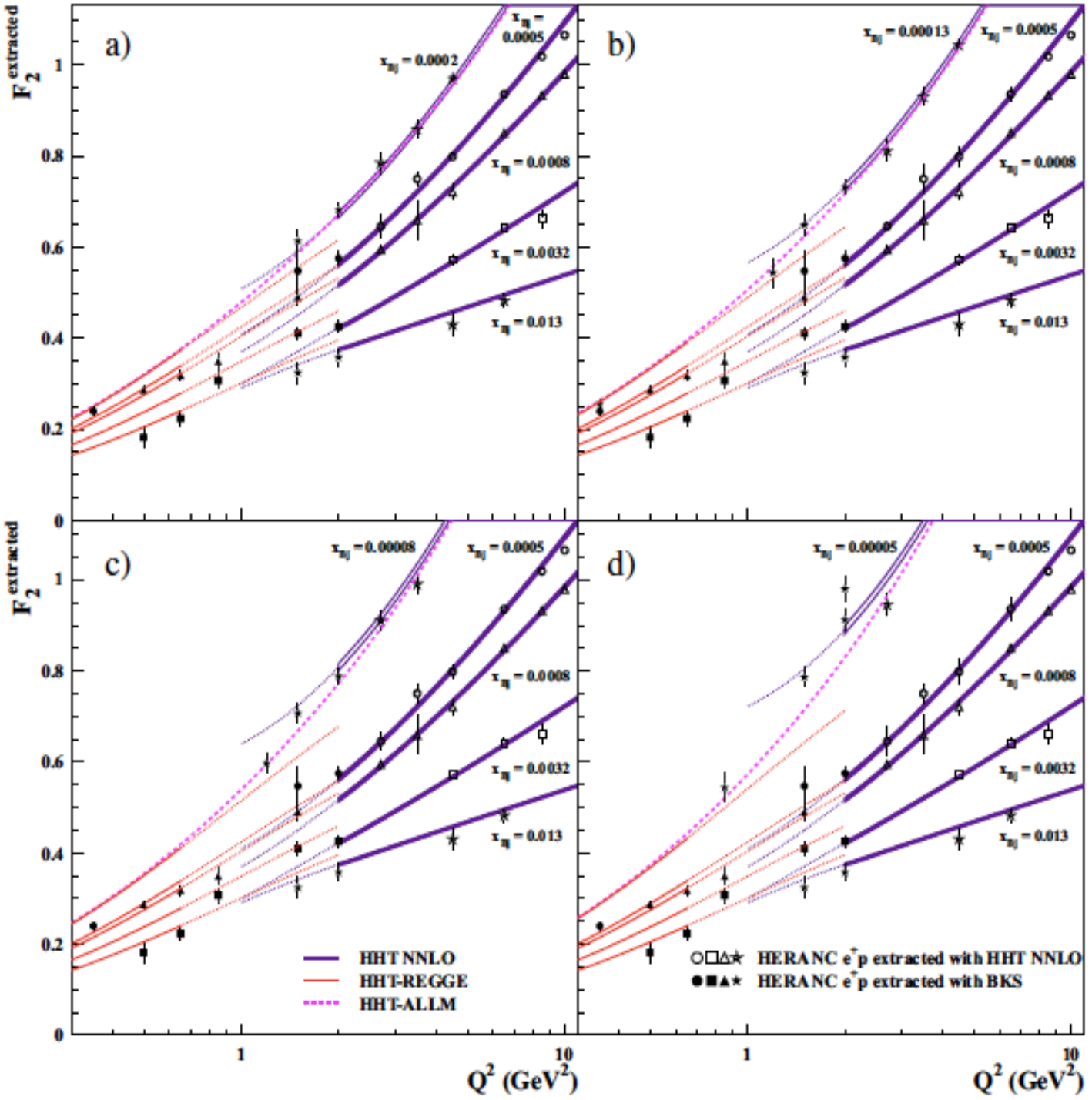
a)
b)
c)
d)
$F_2^{extracted}$
x_{Bj} = 0.0002
x_{Bj} = 0.0005
x_{Bj} = 0.0008
x_{Bj} = 0.0032
x_{Bj} = 0.013
x_{Bj} = 0.00013
x_{Bj} = 0.00008
x_{Bj} = 0.00005
HHT NNLO
HHT-REGGE
HHT-ALLM
HERANC e^+p extracted with HHT NNLO
HERANC e^+p extracted with BKS
Q^2 (GeV^2)

now to ultra-peripheral collisions

Some remarks on ultra-peripheral collisions in p-Pb and Pb-p

3 possibilities in ALICE: Forward, Semi-forward, and Central

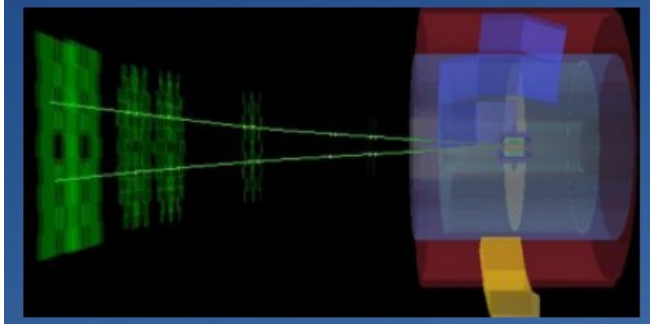

Both muons in muon arm
J/ψ rapidity: -4.0 < y < -2.5
γ+p CM energies:
$21 \leq W_{\gamma p} \leq 45$ GeV (p+Pb)
$550 \leq W_{\gamma p} \leq 1160$ GeV (Pb+p)

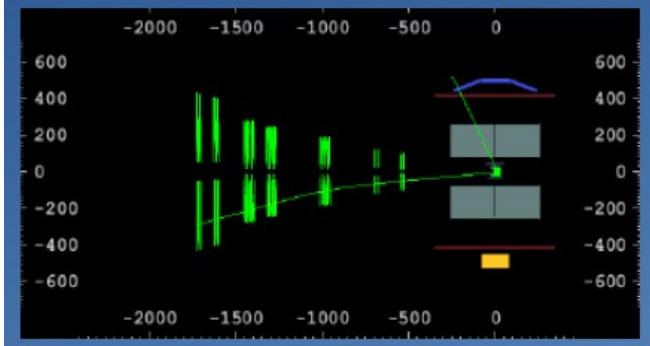

One muon in muon arm, one in central barrel
J/ψ rapidity: -2.5 < y < -1.3
γ+p CM energies:
$45 \leq W_{\gamma p} \leq 82$ GeV (p+Pb)
$300 \leq W_{\gamma p} \leq 550$ GeV (Pb+p)

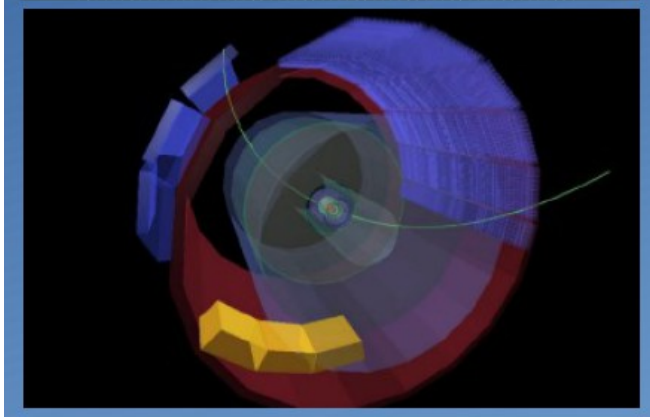

Both muons/electrons in central barrel
J/ψ rapidity: -0.9 < y < 0.9
γ+p CM energies:
$100 \leq W_{\gamma p} \leq 250$ GeV (p+Pb/Pb+p)

$W_{\gamma p}$ - γ-p center of mass energy

2 Pb nuclei collide at 2.76 TeV/nucleon without breaking apart and only 1 lepton pair with invariant mass of the J/psi is produced!

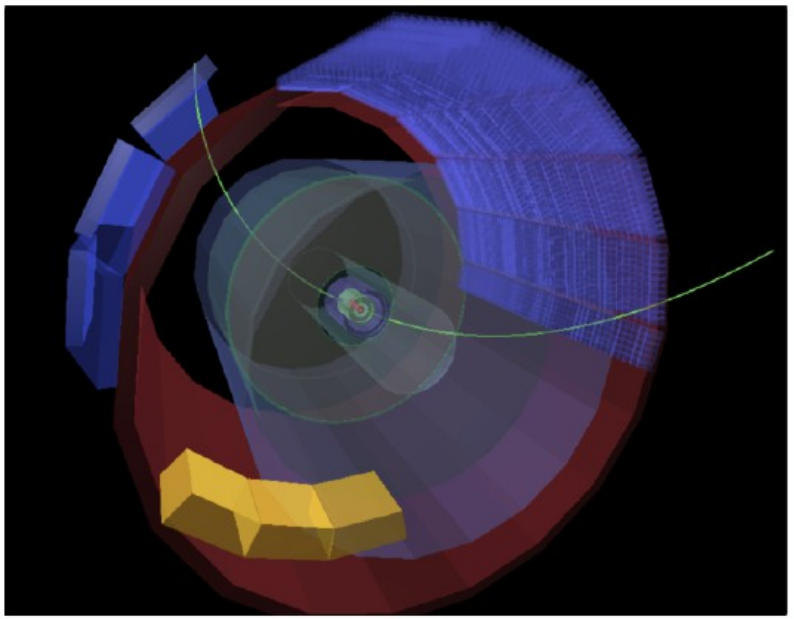

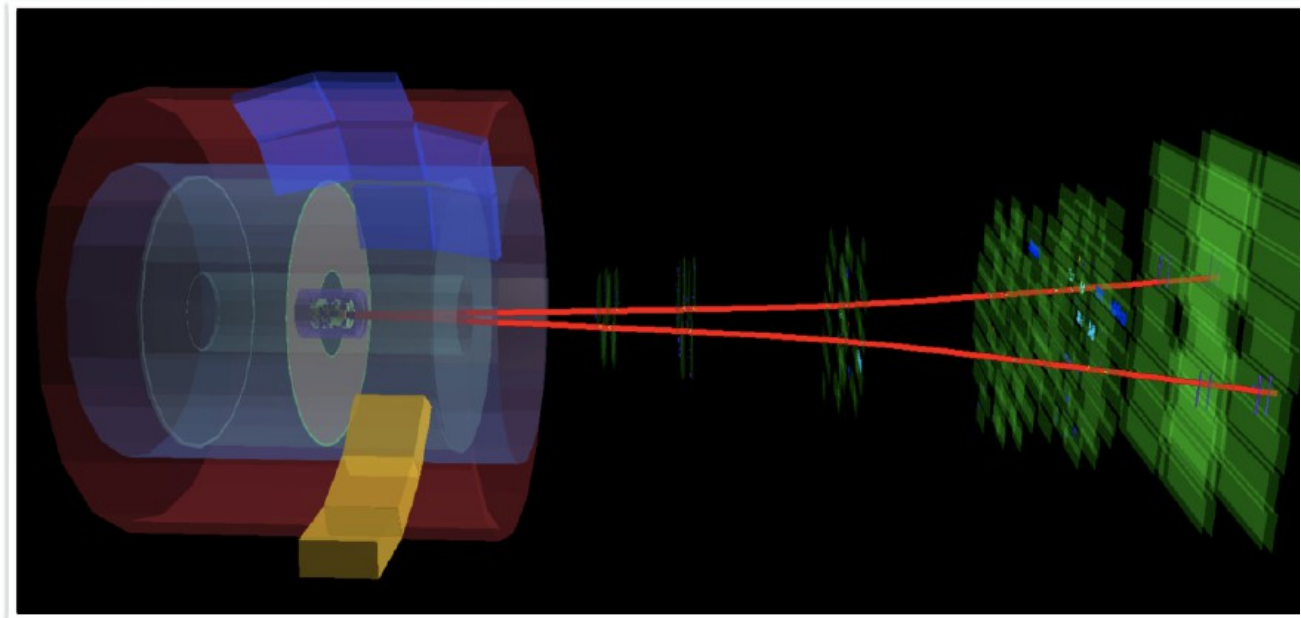

data from the ALICE collaboration

UPC in ALICE p-Pb

For symmetric systems (Pb+Pb/p+p) and $y \neq 0$, one has two contributions:

high E_γ - low x or low E_γ - high x

Not straight forward to separate the two.

⇒ Advantage in p-Pb, photon is almost always emitted by Pb-nucleus.

⇒ Can study γ+p interactions at unprecedented energies at forward rapidities.

$$\omega_{1,2} = \frac{1}{2} M_V e^{\pm y}$$

Ultra-peripheral collisions (UPCs)

- Heavy nuclei carry strong electric and magnetic fields
  - Fields are perpendicular -> treat as nearly-real virtual photons
    - $E_{max} = \gamma hc/b$
  - Photonuclear interactions
  - Two-photon interactions
- Visible when $b>\sim 2R_A$, so there are no hadronic interactions;
  - STAR & ALICE also see photon interactions in peripheral nuclear collisions

Energy	AuAu RHIC	pp RHIC	PbPb LHC	pp LHC
Photon energy (target frame)	0.6 TeV	~12 TeV	500 TeV	~5,000 TeV
CM Energy $W_{\gamma p}$	24 GeV	~80 GeV	700 GeV	~3000 GeV
Max $\gamma\gamma$ Energy	6 GeV	~100 GeV	200 GeV	~1400 GeV

*LHC at full energy $\sqrt{s}$=14 TeV/5.6 TeV

next 4 slides from Spencer Klein, talk at QM2017, Chicago,
see also arXiv:1704.04715

γγ -> Dileptons

- Large samples from ALICE, ATLAS & STAR
- Data is in excellent agreement with lowest order QED
  - STARlight Monte Carlo
  - Zα ~ 0.6, so perturbation theory might fail
- Light-by-light scattering seen by ATLAS
  - Sensitive to new particles

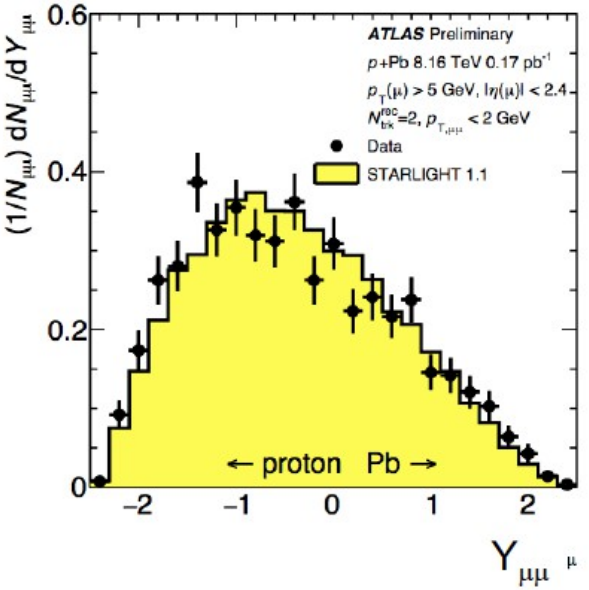

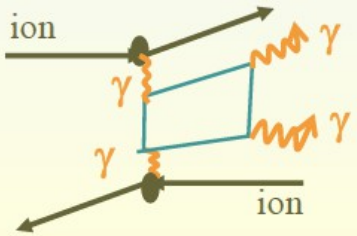

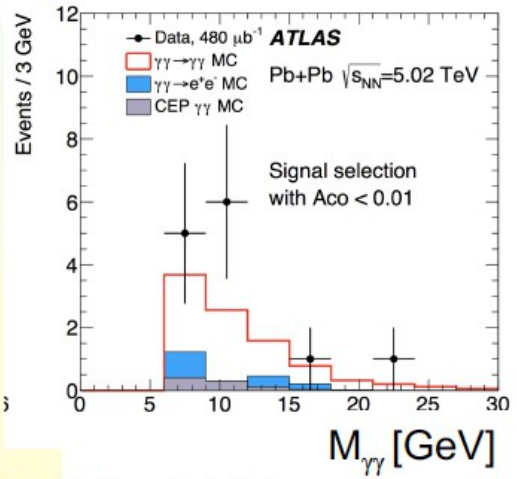

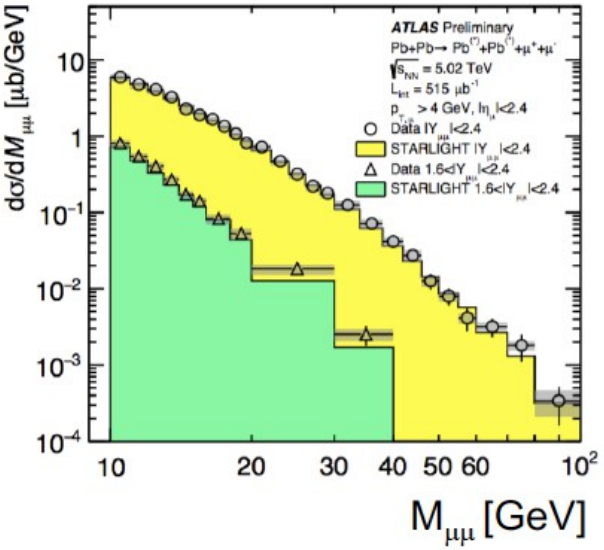

ATLAS: arXiv:1702.01625; M. Dyndal, this conference

VM photoproduction in pQCD

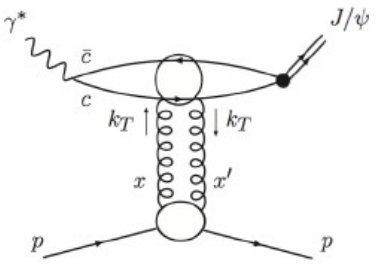

- In 2-gluon model, leading order pQCD

$$\frac{\mathrm{d}\sigma}{\mathrm{d}t}\left(\gamma^* p \to J/\psi\, p\right)\Big|_{t=0} = \frac{\Gamma_{ee} M_{J/\psi}^3 \pi^3}{48\alpha}\left[\frac{\alpha_s(\bar{Q}^2)}{\bar{Q}^4} x g(x,\bar{Q}^2)\right]^2 \left(1+\frac{Q^2}{M_{J/\psi}^2}\right).$$

- With $\bar{Q}^2 = (Q^2 + M_{J/\psi}^2)/4, \qquad x = (Q^2 + M_{J/\psi}^2)/(W^2 + Q^2)$
  - Vector meson mass provides hard scale
- Some caveats
  - pQCD factorization does not strictly hold
    - Two gluons have different x values (with x' ≪ x ≪ 1)
      - Use generalized (skewed) gluon distributions – smallish correction.
      - Can do exactly with Shuvaev transform
  - Photon is not pure $q\bar{q}$ dipole
  - Choice of scale μ
  - "Absorptive corrections" for pp akin to $b > R_A + R_b$

Jones, Martin, Ryskin and Teubner ("JMRT"), JHEP 1311, 085 (2013); and others

σ(γp-> J/ψ p)

- Data up to $W_{\gamma p}$= 1.5 TeV -5 times the HERA maximum
- ALICE sees good pA agreement with HERA data
- LHCb 13 TeV-beam data somewhat below 7 TeV data?
  - LHCb uses bootstraps from HERA range for 2-fold ambiguity
- NLO calculation predicts a small down-turn from power law prediction at energies above ~ 300 GeV
  - 13 TeV data agrees well with NLO calculation

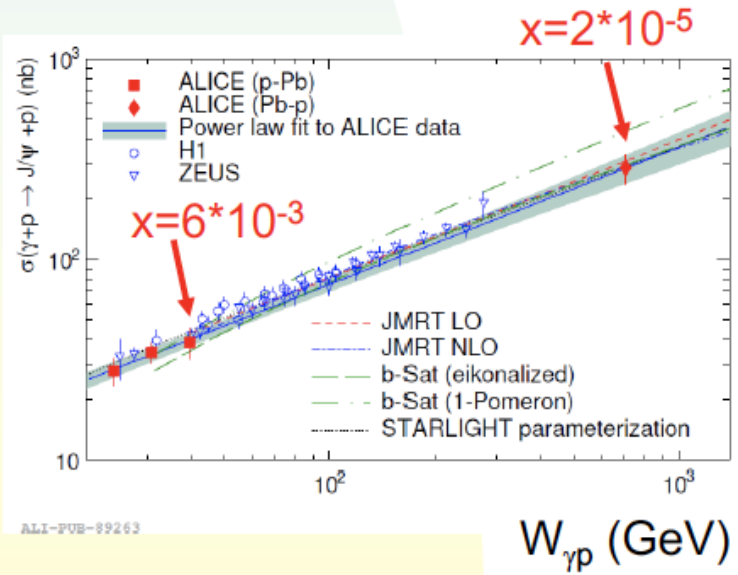

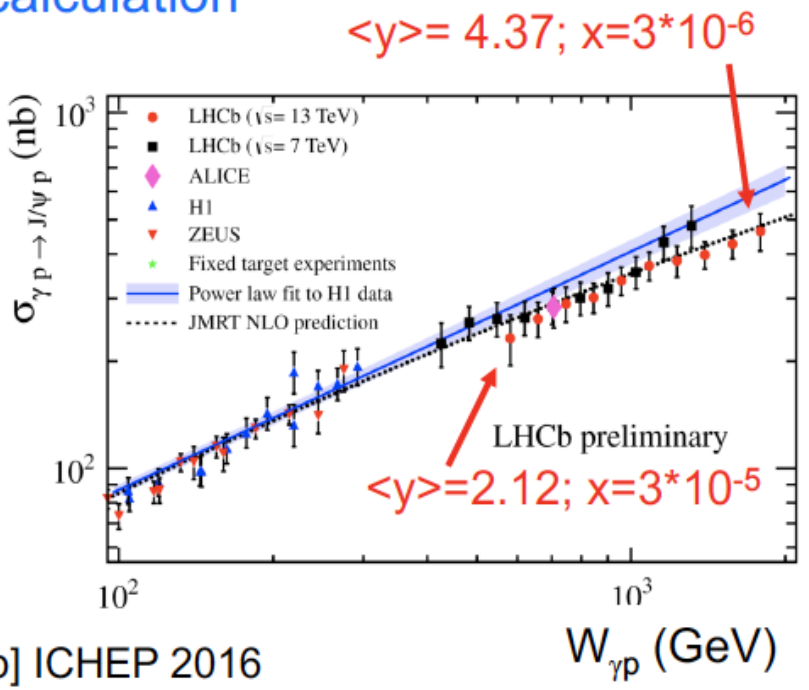

J. Adams [ALICE], DIS 2016; R. McNulty [LHCb] ICHEP 2016

power law exponent delta essentially unchanged down to x = 3*10^{-6}
no evidence yet for anomalous W dependence over full x range

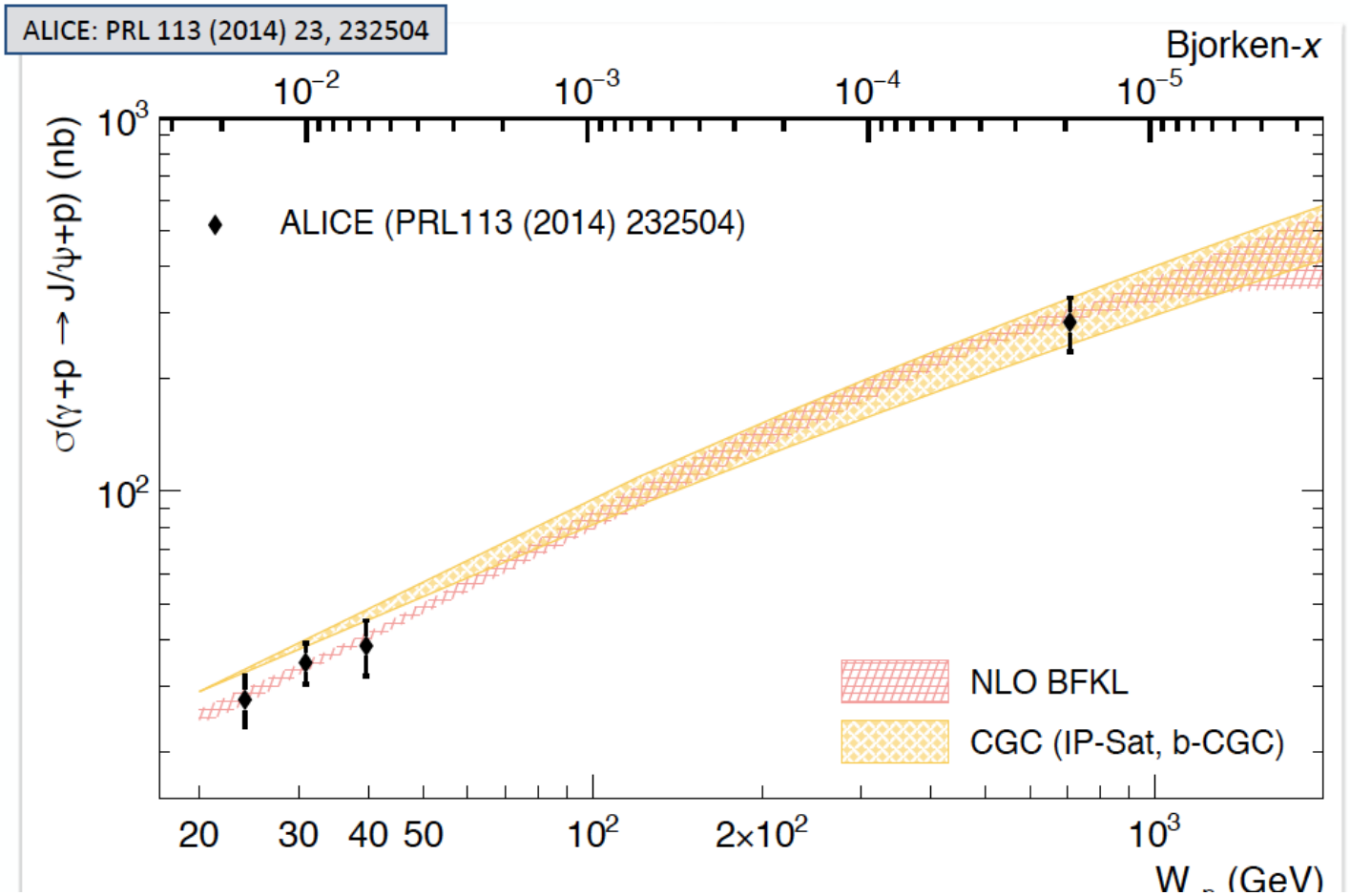

- ALICE data are also correctly described by recent calculations using:
  - CGC by Armesto and Rezaeian Phys.Rev. D90 (2014) 054003,
  - NLO BFKL by Bautista et el Phys.Rev. D94 (2016) 054002.

Figure from J.G. Contreras, EMMI workshop, Krakow, Poland, Sep. 2017

ALICE: PRL 113 (2014) 23, 232504

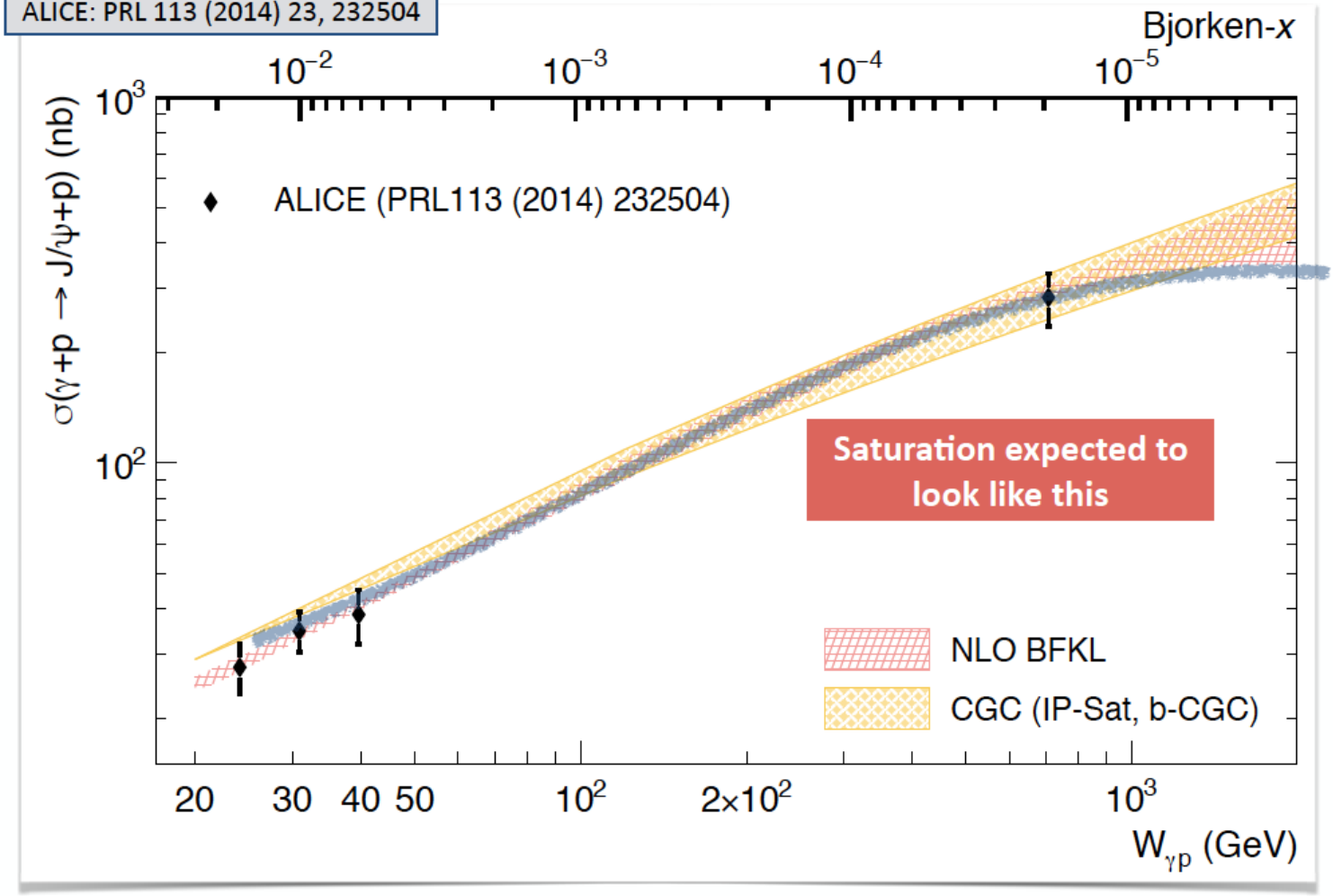

Energy dependence of dissociative J/ψ photoproduction as a signature of gluon saturation at the LHC

J. Cepila, J.G. Contreras (Prague, Tech. U.),
J. D. Tapia Takaki (Kansas U.). Aug 26, 2016. 6 pp.

Published in Phys.Lett. B766 (2017) 186-191

We have developed a model in which the quantum fluctuations of the proton structure are characterised by hot spots, whose number grows with decreasing Bjorken- x . Our model reproduces the F2(x,Q2) data from HERA at the relevant scale, as well as the exclusive and dissociative J/ψ photoproduction data from H1 and ALICE. Our model predicts that for Wγp≈500 GeV , the dissociative J/ψ cross section reaches a maximum and then decreases steeply with energy, which is in qualitatively good agreement to a recent observation that the dissociative J/ψ background in the exclusive J/ψ sample measured in photoproduction by ALICE decreases as energy increases. Our prediction provides a clear signature for gluon saturation at LHC energies.

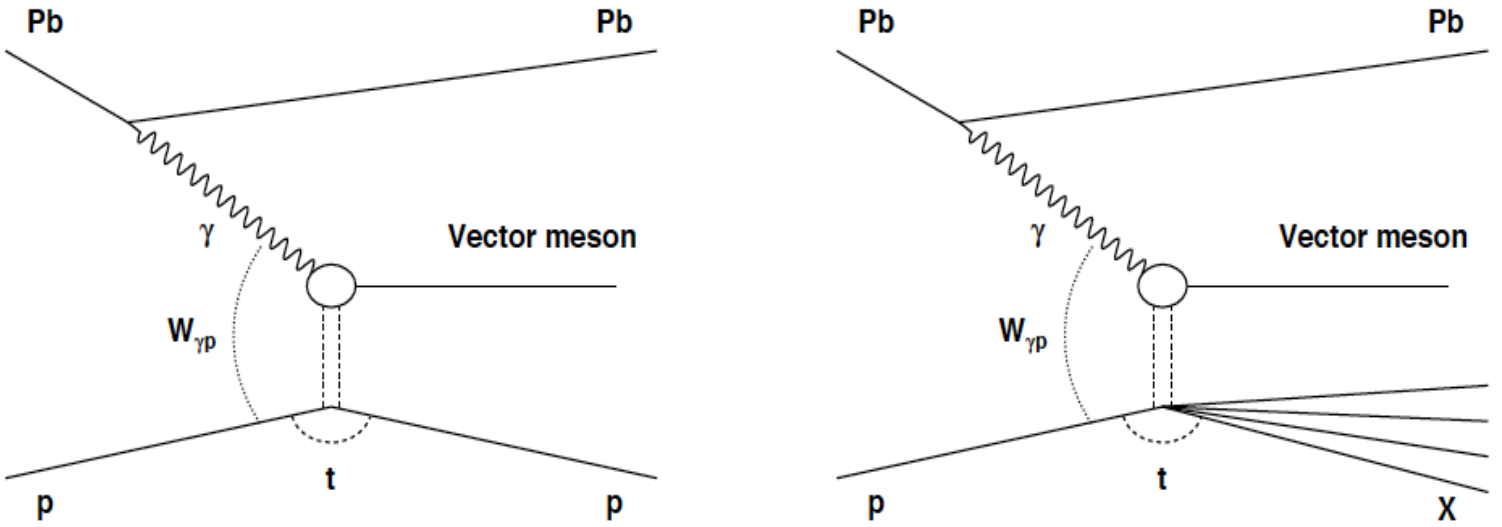

Figure 1: Diagrams for exclusive (left) and dissociative (right) vector meson photoproduction. The source of photons is a lead nucleus as in p-Pb collisions at the LHC. For the case of HERA, the source of photons was either an electron or a positron.

the model

the color dipole interacts with the nucleus according to the Golec-Biernat/Wuesthoff 'saturation model

$$N(x,r,b) = \sigma_0 N(x,r) T(\vec{b})$$

$$N(x,r) = \left(1 - e^{-r^2 Q_s^2(x)/4}\right),$$

with the saturation scale given by

$$Q_s^2(x) = Q_0^2 (x_0/x)^{\lambda},$$

new approach: the proton profile function T(b) contains regions of 'hot spots' which are introduced according to:

$$N_{hs}(x) = p_0 x^{p_1} (1 + p_2 \sqrt{x})$$

this x dependence introduces an implicit W dependence!

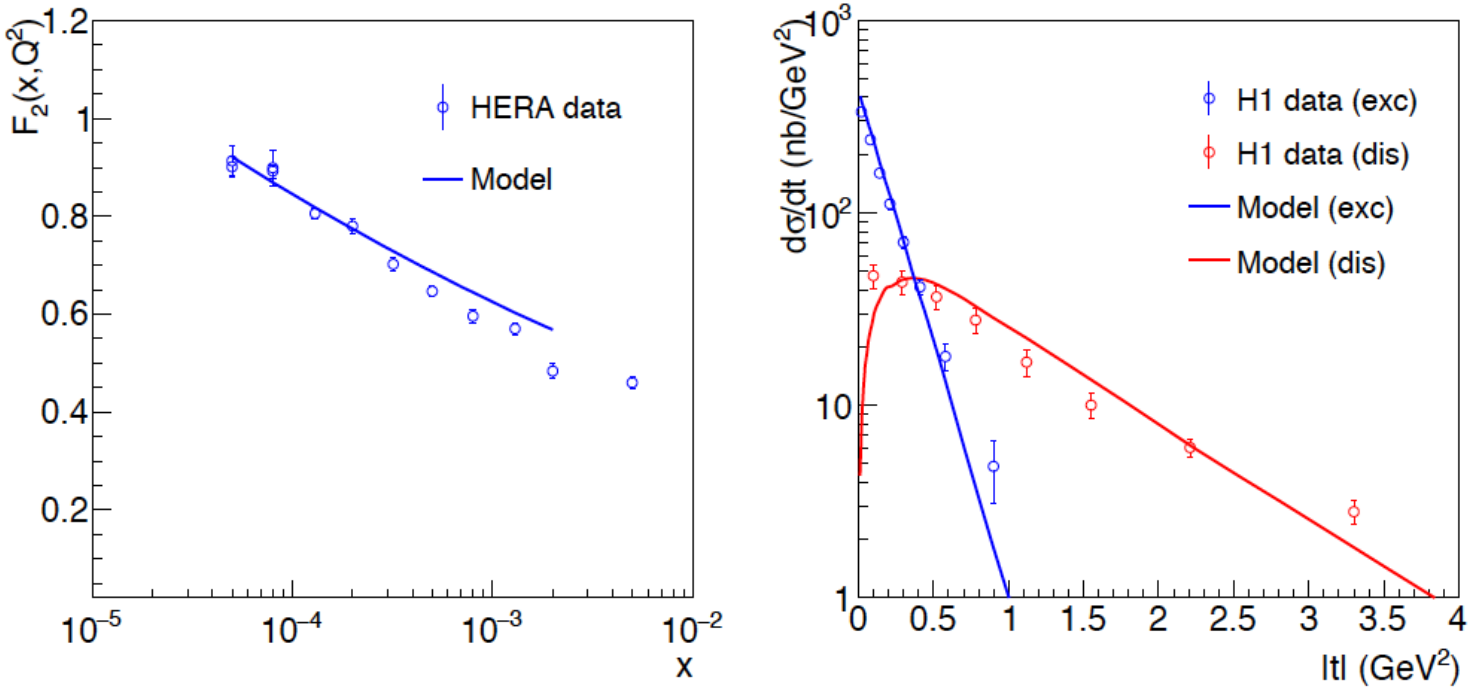

Figure 2: Comparison of the model (solid lines) to data (open bullets) on (left) the structure function of the proton $F_2(x, Q^2)$ at $Q^2 = 2.7$ GeV^2 as measured by H1 and Zeus [26] and (right) the $|t|$ distribution of exclusive (blue) and dissociative (red) photoproduction of J/ψ as measured by H1 [11] at $\langle W_{\gamma p} \rangle = 78$ GeV.

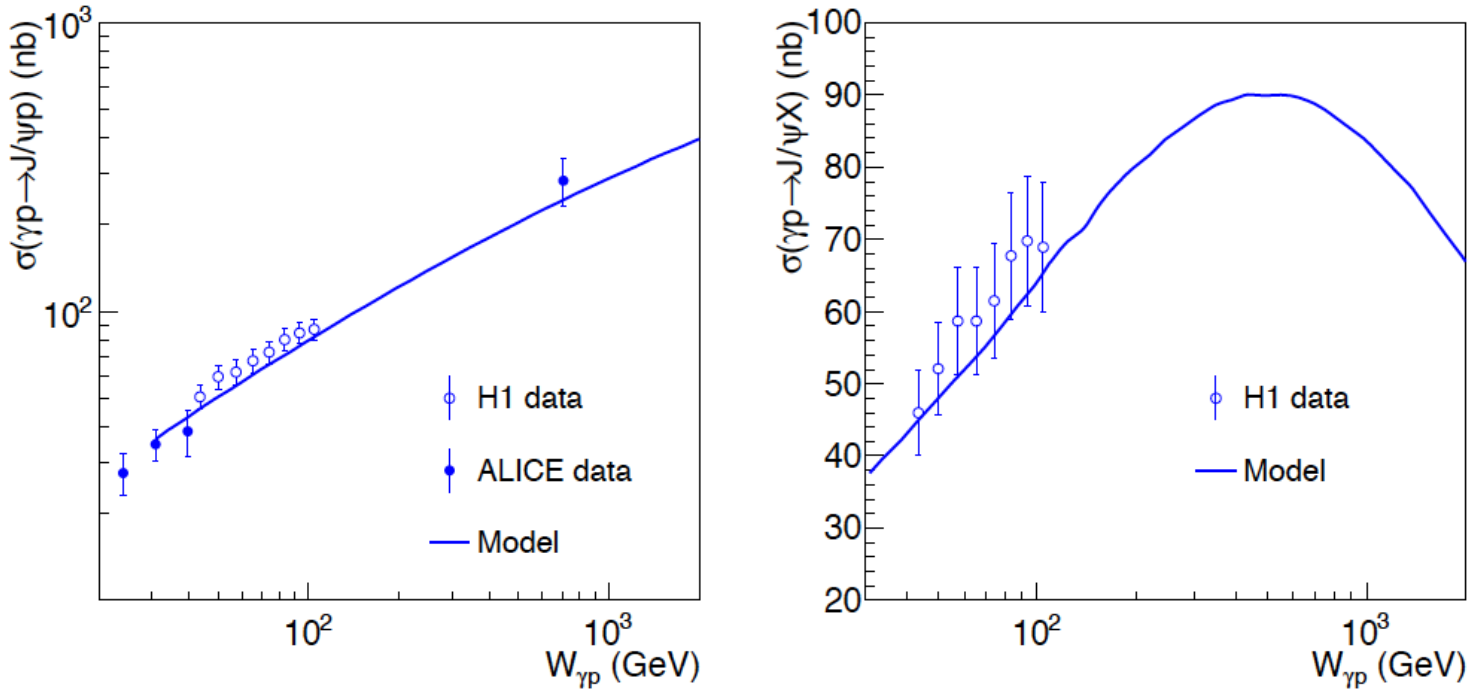

Figure 3: Comparison of the model (solid lines) to data on the $W_{\gamma p}$ dependence of the cross section for exclusive (left) and dissociative (right) photoproduction of J/ψ as measured by H1 [11] and ALICE [6] (open and solid bullets, respectively).

observation of this peak would be, in this model, a consequence of saturation – is this unique?

Shadowing extracted from J/psi production in UPC Pb-Pb vs pp

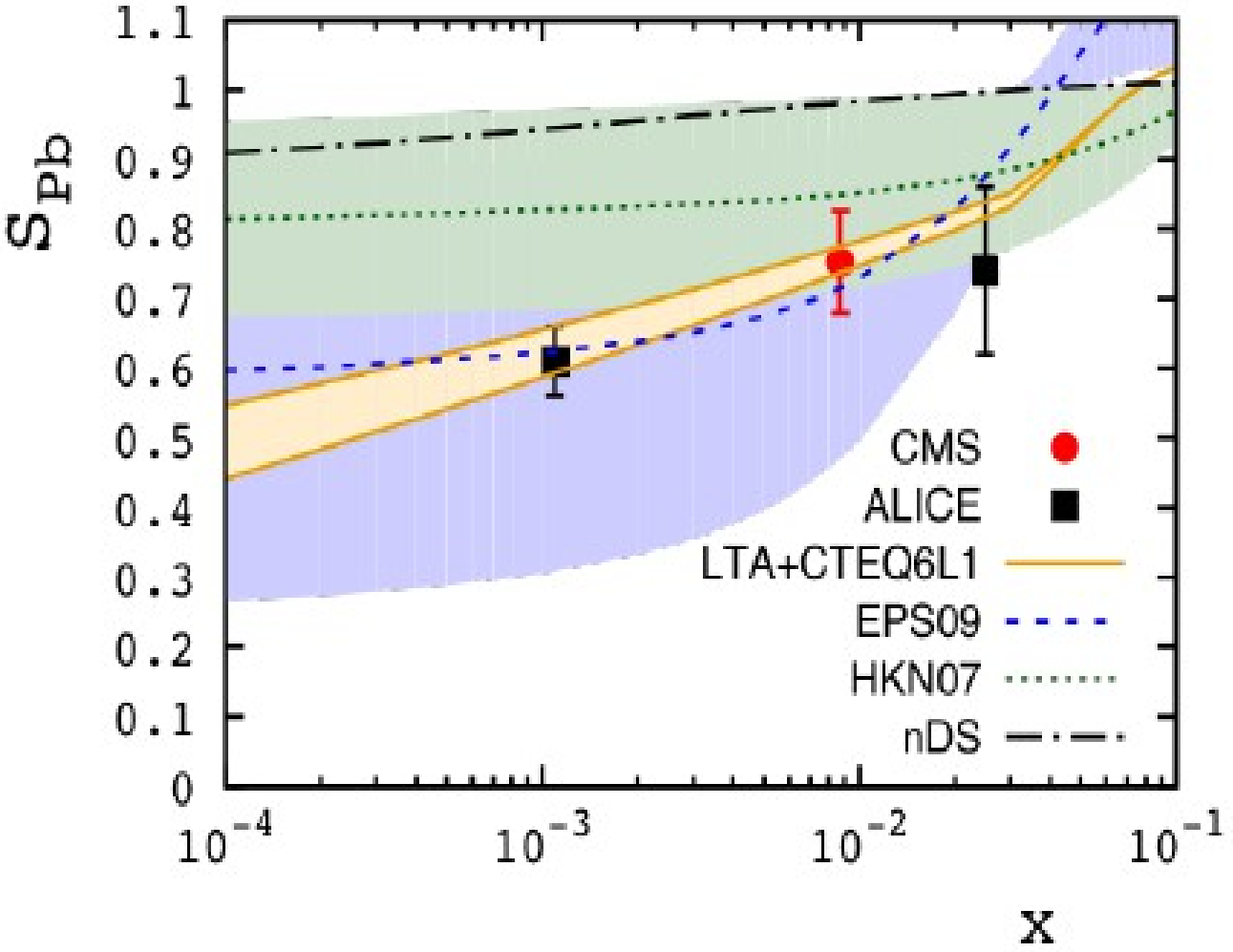

Results constrain EPS09 shadowing calculations and agree with recent leading twist (LTA) calculations. Fig. Taken from Vadim Guzey V. Guzey and M. Zhalov, JHEP **1310**, 207 (2013)

LHC reach for gluon distributions in nuclei from ultra-peripheral collision studies

Fig. taken from Baltz et al., Phys. Reports 458 (2008)1 with the additional domain opened by p-Pb collisions

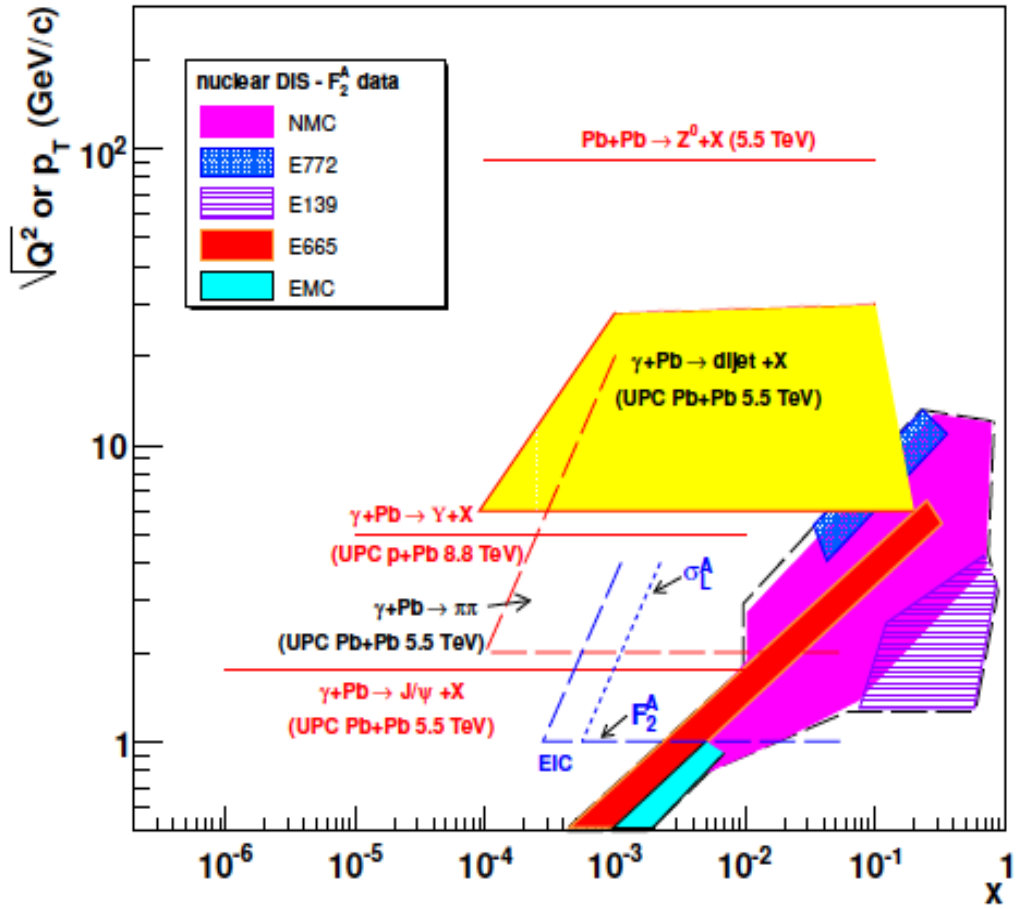

precision measurement of open charm production by LHCb measurement at forward rapidity provides input on low-x gluon PDFs

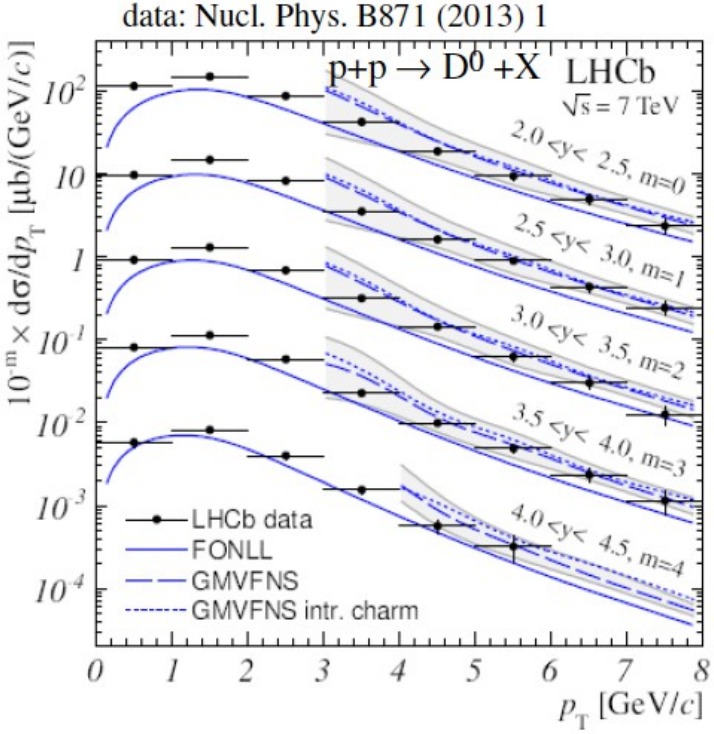

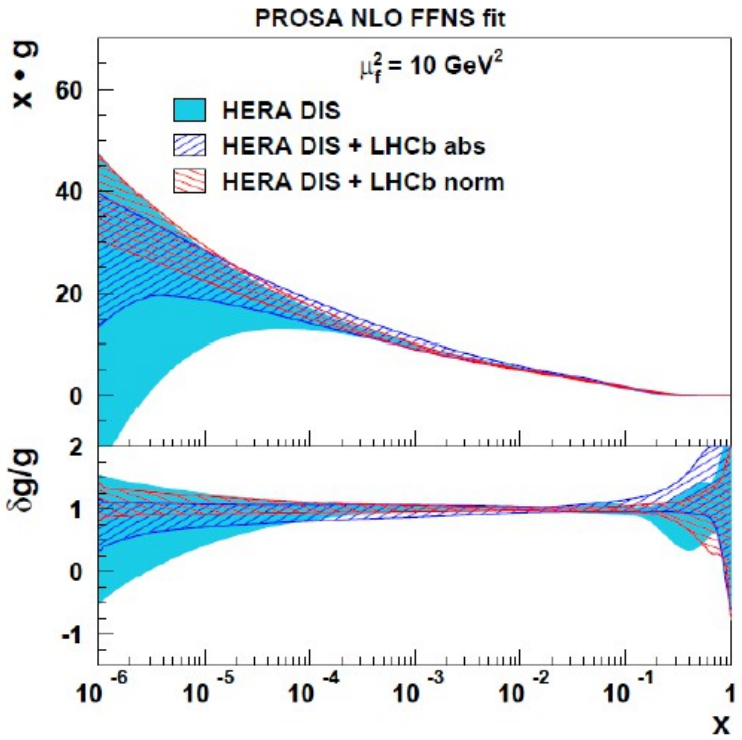

for a recent summary of data and pQCD predictions see:
Guzzi, Geiser, Rizatdinova, 1509.04582 and Beraudo, 1509.04530
additional constraint of gluon PDF in particular at low x (down to 5 10^{-6})

new analysis by Gauld, Rojo and Slate, arXiv:1705.04217

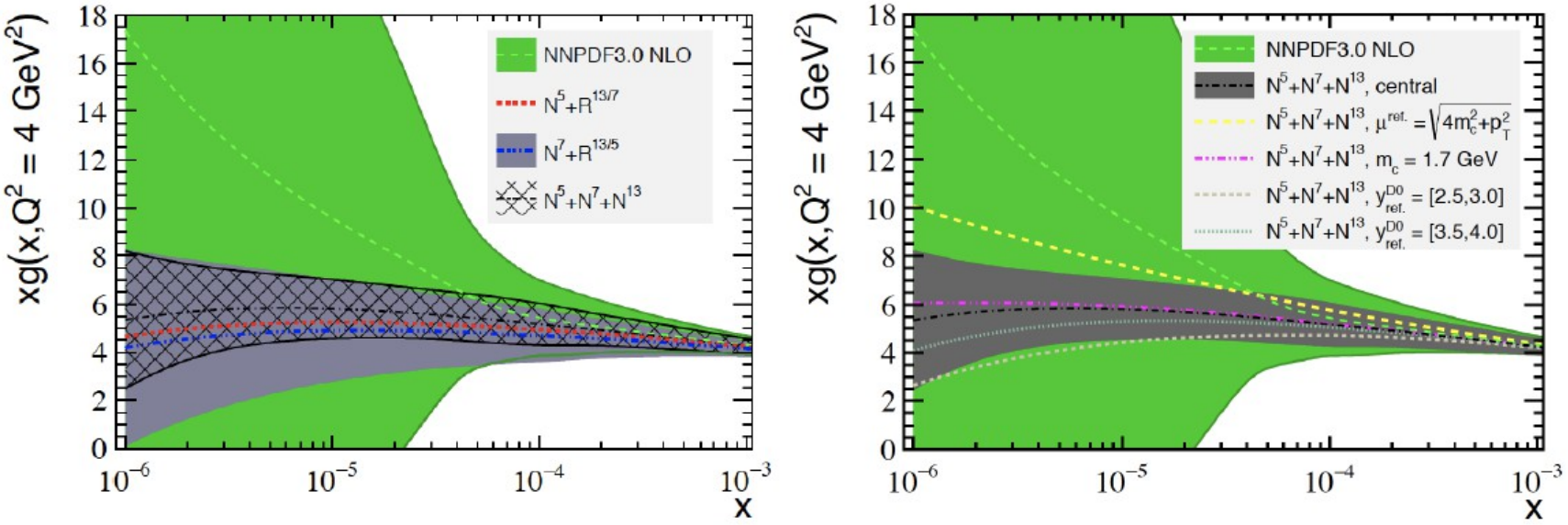

Figure 1: Left plot: the small-x gluon PDF in NNPDF3.0 compared with the results when various combinations of LHCb D meson production data are included in the fit. Right plot: the impact of variations of the input theoretical settings in the $N^5 + N^7 + N^{13}$ NNPDF3.0+LHCb fit.

good constraints down to x = 10^{-6} by analysis of LHCb pp ► D at 5, 7, 13 TeV data

backup slides

LHC ion program for Run3 and Run4

Main conclusion of the '2013 European Strategy for Particle Physics' process

"Europe's top priority should be the exploitation of the full potential of the LHC, including the high-luminosity upgrade of the machine and detectors with a view to collecting ten times more data than in the initial design, by around 2030. This upgrade programme will also provide further exciting opportunities for the study of flavour physics ***and the quark-gluon plasma."***

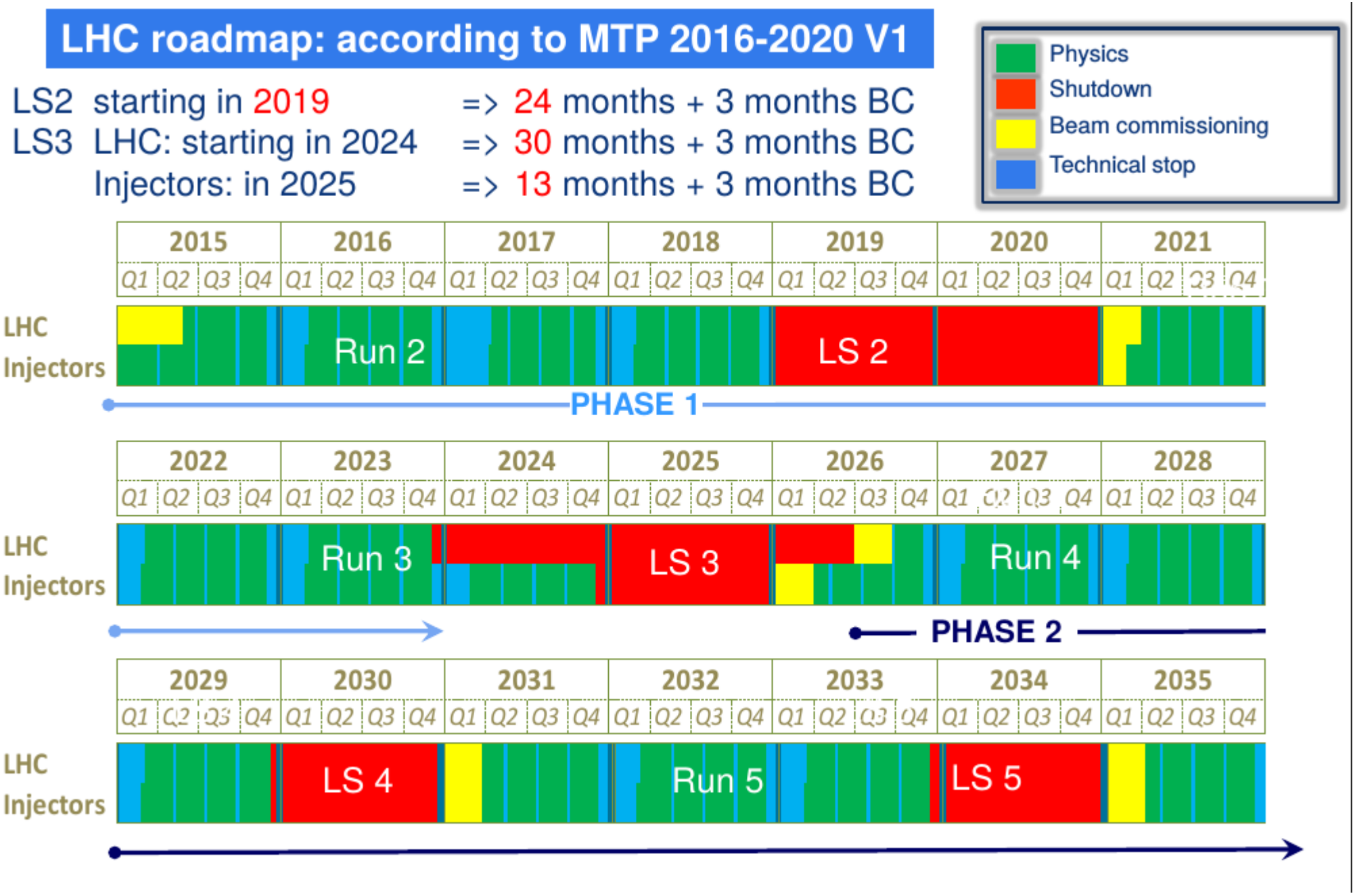

approved ALICE program up to and including LHC Run4

ALICE Upgrade Strategy

High precision measurements of rare probes at low $p_{T,}$ which cannot be selected with a trigger, require a large sample of events recorded on tape

Target

- Pb-Pb recorded luminosity ≥ 10 nb^{-1} ➡ 8 x 10^{10} events
- pp (@5.5 Tev) recorded luminosity ≥ 6 pb^{-1} ➡ 1.4 x 10^{11} events

Gain a factor **100** in statistics over approved programme

… and significant improvement of vertexing and tracking capabilities

I. Upgrade the ALICE readout systems and online systems to

- read out all Pb-Pb interactions at a maximum rate of 50kHz (i.e. L = 6x10^{27} $cm^{-1}s^{-1}$), with a minimum bias trigger → NEW GEM TPC Readout Planes
- Perform online data reduction based on reconstruction of clusters and tracks (tracking used only to filter out clusters not associated to reconstructed tracks)

II. Improve vertexing and tracking at low p_T ➔ NEW ITS

ALICE upgrade: main physics topics for Run3 and Run4

rare probes at low p_T:

- heavy flavor hadrons
- quarkonia
- di-leptons at low and intermediate mass
- light anti-matter and exotic clusters
- jet physics
- event-by-event fluctuations of conserved quantum numbers
- ultra-peripheral collisions , low x physics, photon-photon collisions